Electronic Supplementary Material (ESI) for Energy & Environmental Science.

Supporting Information for:

Carbene Iridium Complexes for Efficient Water Oxidation: Scope and Mechanistic Insights

James A. Woods, † Ralte Lalrempuia,‡ Ana Petronilho,‡ Neal D. McDaniel,† Helge Müller-Bunz,‡ Martin Albrecht,*‡ Stefan Bernhard*†

Department of Chemistry, Carnegie Mellon University, Pittsburgh, Pennsylvania 15213, United States
School of Chemistry & Chemical Biology, University College Dublin, Belfield, Dublin 4, Ireland

† Carnegie Mellon University

‡ University College Dublin

Contents:

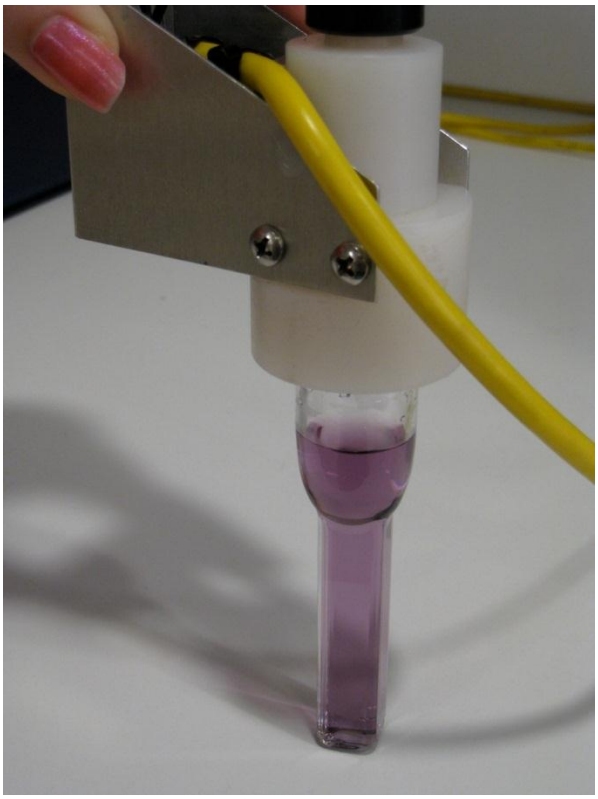

Figure S1: Aqueous solution of **4c** (0.5 mM in 1N HNO_3) after 8 additions of 20 equivalents ceric ammonium nitrate. Reaction vessel was well mixed throughout. Cuvette vial allows concurrent manometry and visible spectroscopy.

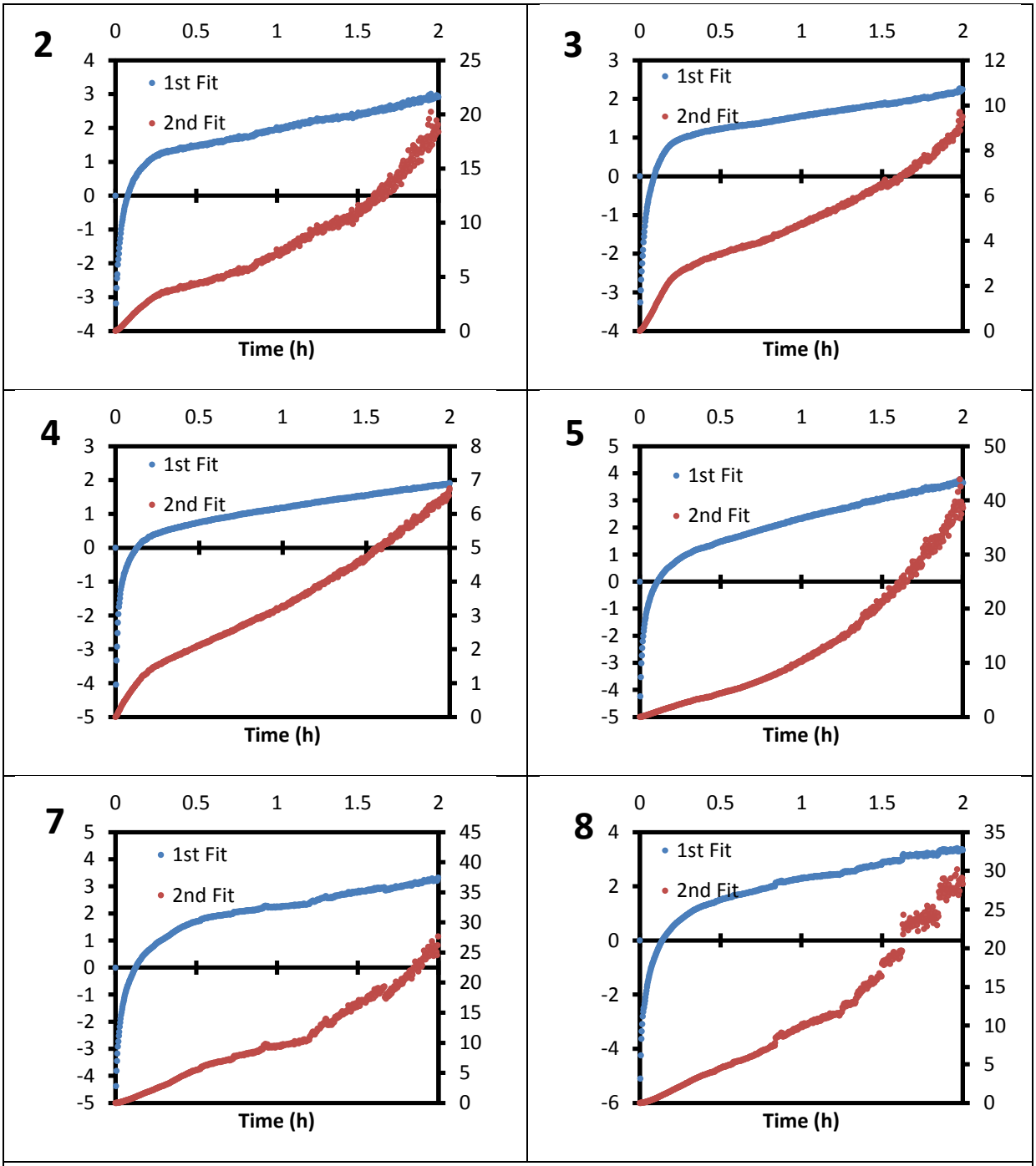

Figure S2: From experiment described in Figure 5: First Order (blue, left axis) and Second Order (red, right axis) linearizations of cerium(IV) additions 2, 3, 4, 5, 7, and 8 (Left to right, top to bottom) in hours. First order linearizations are plotted as $ln\left(\frac{mol\ O_2(t)}{Max\ O_2 - mol\ O_2(t)}\right)$ vs. time in hours while second order linearizations are plotted as $\frac{mol\ O_2(t)}{Max\ O_2 - mol\ O_2(t)}$ vs. time in hours. First order plots are linear in the second stage of the reaction (after 30 min) while at the beginning, second order plots are linear, indicating a change of reaction order.

Figure S3a: Experimental oxygen evolution traces from the initial 50 hours of the experiment described in **Figure 3** and fitted traces per Scheme 4 (Solid line, markers respectively). Note the close agreement of the fitted and experimental data even at the initial phase where a single or double exponential would fail.

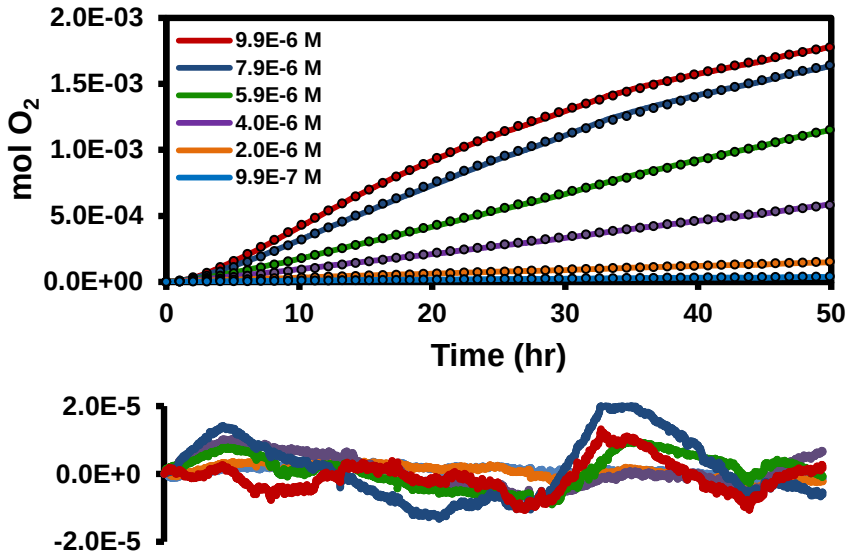

Figure S3b:
Residual error between experimental traces and calculated traces. All six reactions were run simultaneously; note the generally larger cyclical systematic error in the more productive reactions. *Despite the use of a water-jacketed sample holder, the concurrent cyclical systematic error in this figure is largely the result of the diurnal response to heating and cooling by the building HVAC system – Note the magnitude of error relative to the response.*

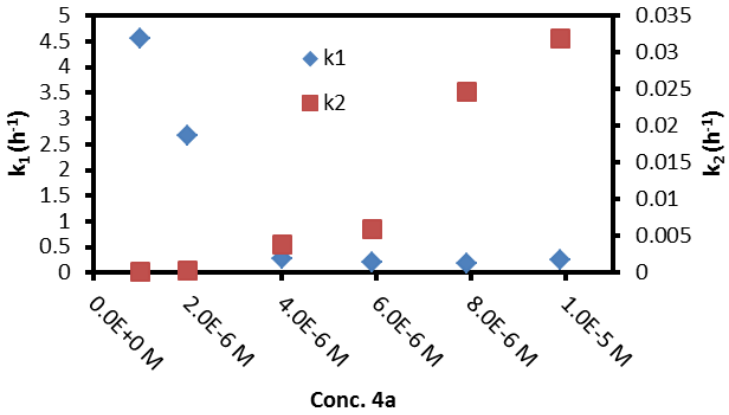

Figure S3c:
Rate constants determined by least-squares regression indicating a nonlinear changes of both first and second order rate constants

Figure S3d: Log-Log plot of **4a** Rate vs. concentration.

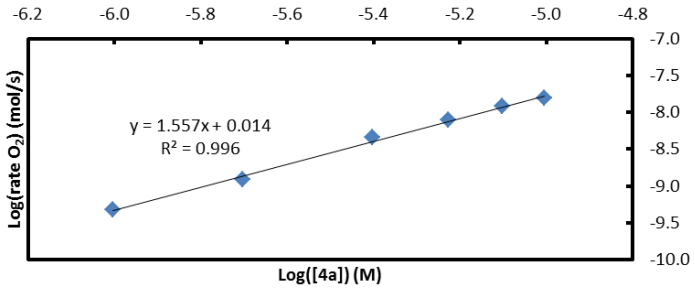

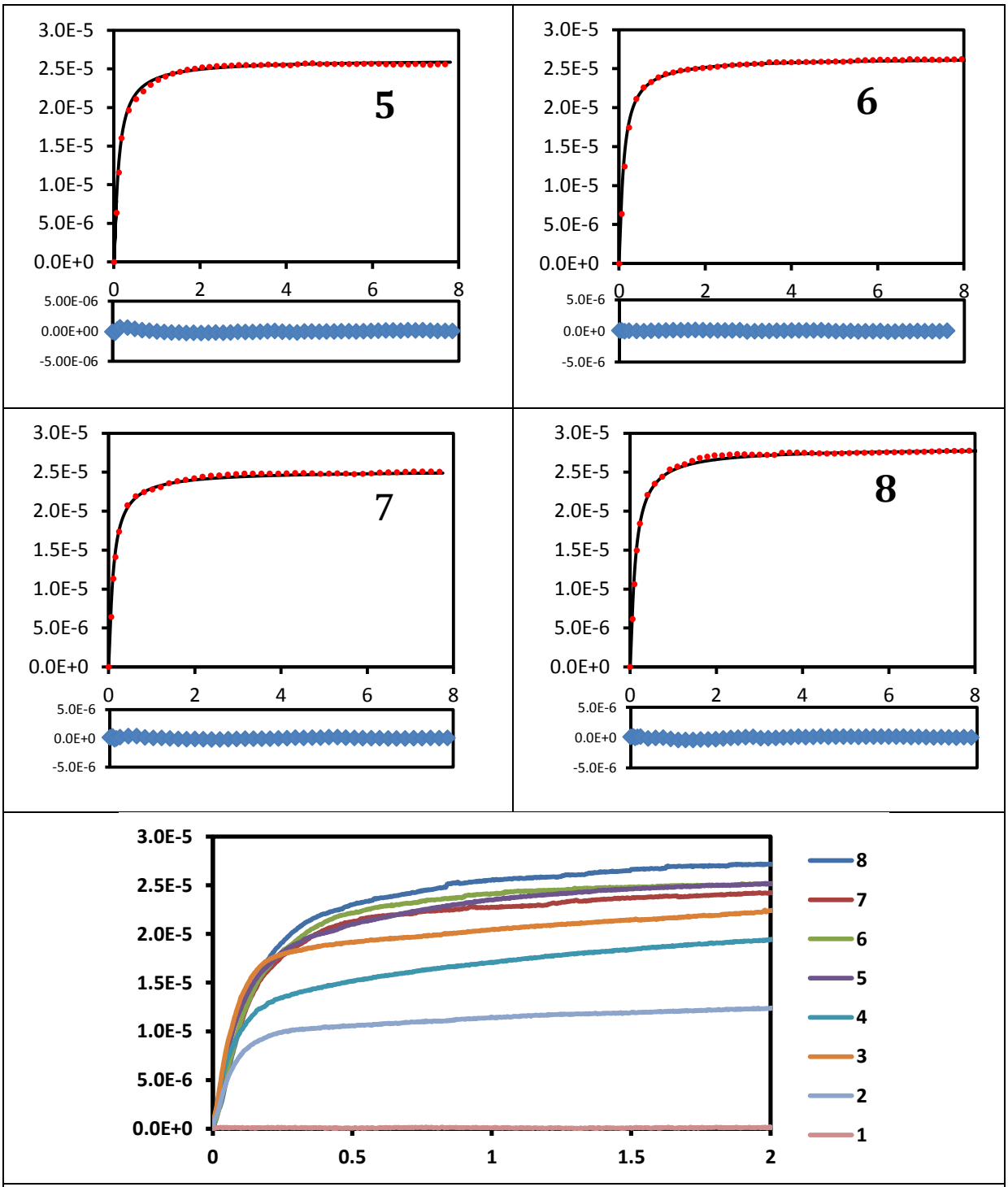

Figure S4: Top: Agreement of fitted with measured data points.fits employing sequential first order reactions (Scheme 4) of additions 5, 6, 7, and 8 (abscissa: hours, ordinate: moles of dioxygen). **Bottom:** Alternative view of Figure 5 featuring superimposed oxygen evolution traces from the 8 consecutive additions of cerium(IV), indicating the gradual increase of oxygen production over the first four steps.

Step	FIT: A (mol)	FIT: K1 (h-1)	FIT: K2 (h-1)	SSE
6	2.651E-05	32.70	13.98	2.888E-12

Time (h)	Exp. O2 (mol)	Calc. O2 (mol)	Time (h) (cont.)	Exp. O2 (mol)	Calc. O2 (mol)
0.046	5.045E-06	6.185E-06	1.186	2.444E-05	2.437E-05
0.103	1.117E-05	1.204E-05	1.243	2.450E-05	2.447E-05
0.160	1.499E-05	1.537E-05	1.300	2.470E-05	2.455E-05
0.217	1.728E-05	1.747E-05	1.357	2.468E-05	2.463E-05
0.274	1.873E-05	1.891E-05	1.414	2.474E-05	2.470E-05
0.331	2.003E-05	1.995E-05	1.471	2.474E-05	2.477E-05
0.388	2.098E-05	2.075E-05	1.528	2.484E-05	2.483E-05
0.445	2.176E-05	2.137E-05	2.042	2.515E-05	2.523E-05
0.502	2.215E-05	2.187E-05	2.556	2.543E-05	2.548E-05
0.559	2.254E-05	2.228E-05	3.013	2.562E-05	2.563E-05
0.616	2.286E-05	2.263E-05	3.527	2.580E-05	2.576E-05
0.673	2.303E-05	2.292E-05	4.041	2.585E-05	2.585E-05
0.730	2.319E-05	2.317E-05	4.556	2.590E-05	2.593E-05
0.787	2.350E-05	2.339E-05	5.071	2.596E-05	2.598E-05
0.844	2.360E-05	2.358E-05	5.529	2.617E-05	2.603E-05
0.901	2.378E-05	2.375E-05	6.044	2.620E-05	2.607E-05
0.958	2.404E-05	2.390E-05	6.559	2.604E-05	2.610E-05
1.015	2.416E-05	2.404E-05	7.018	2.626E-05	2.613E-05
1.072	2.433E-05	2.416E-05	7.534	2.615E-05	2.615E-05
1.129	2.442E-05	2.427E-05	7.990	2.620E-05	2.617E-05

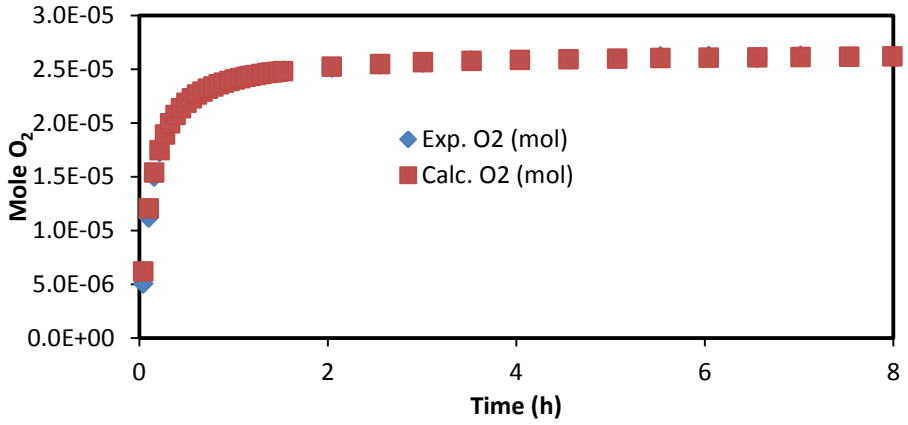

Figure S5: Least squares fit of the data of an example step (6) reduced in length for brevity to illustrate fitting process. Actual data is typically sampled every 5 seconds for ca. 5500 data points per step.

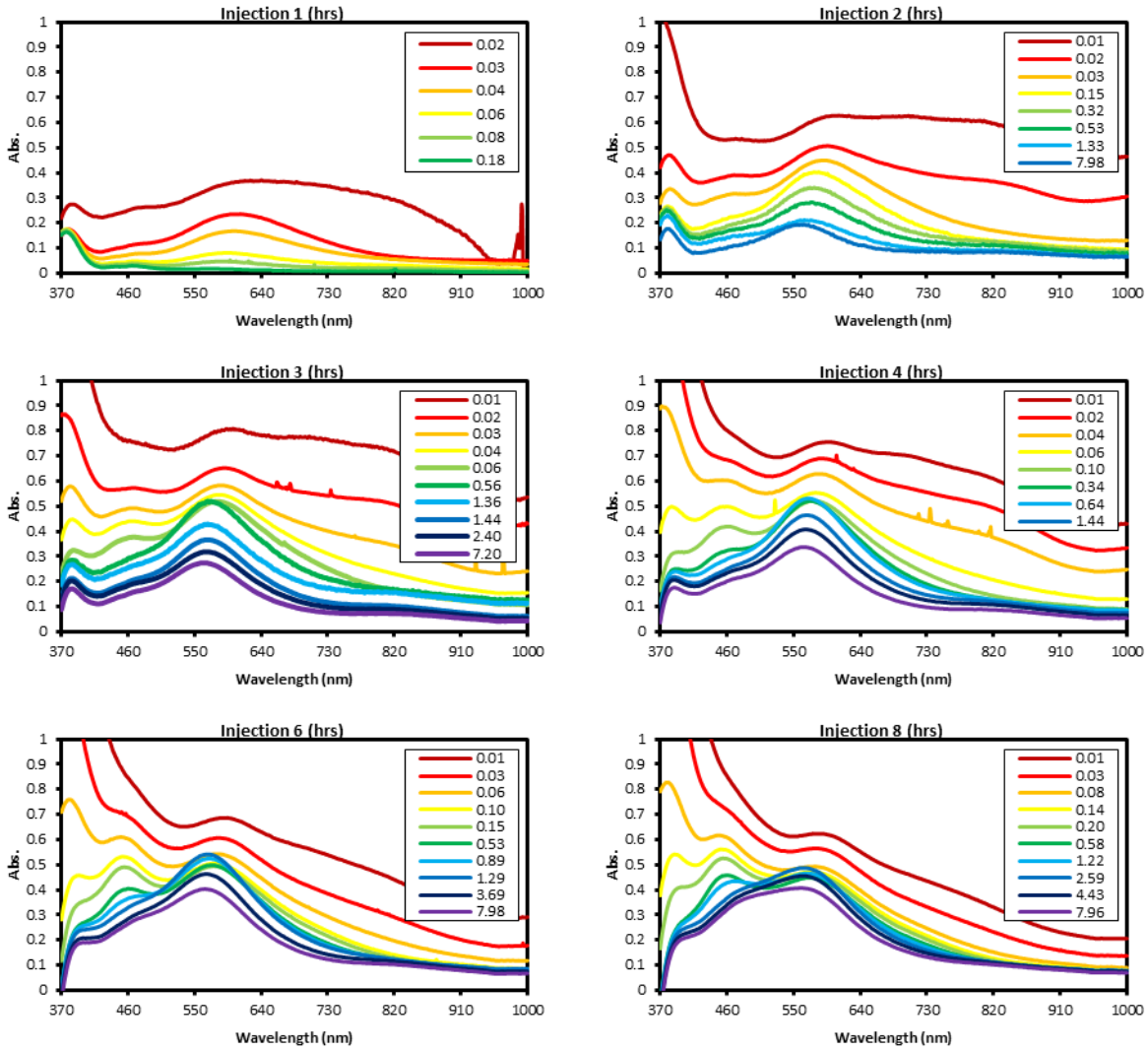

Figure S6: UV-vis absorption spectra of an aqueous solution of **4a** after regular sequential additions of cerium(IV).

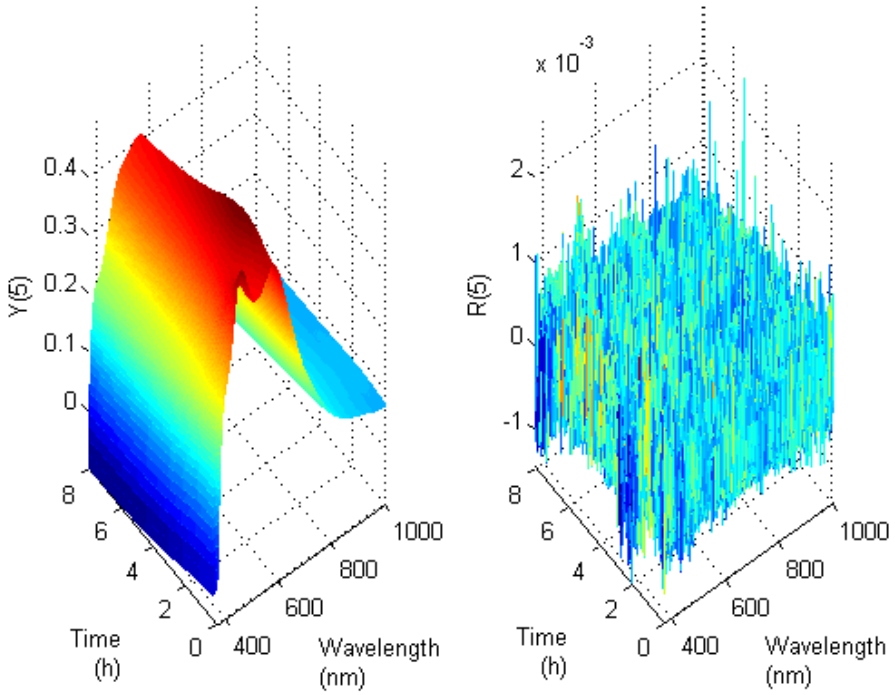

Figure S7: Reconstructed wavelength-time matrix of injection 8 using the singular values identified as significant (left) and insignificant (right).

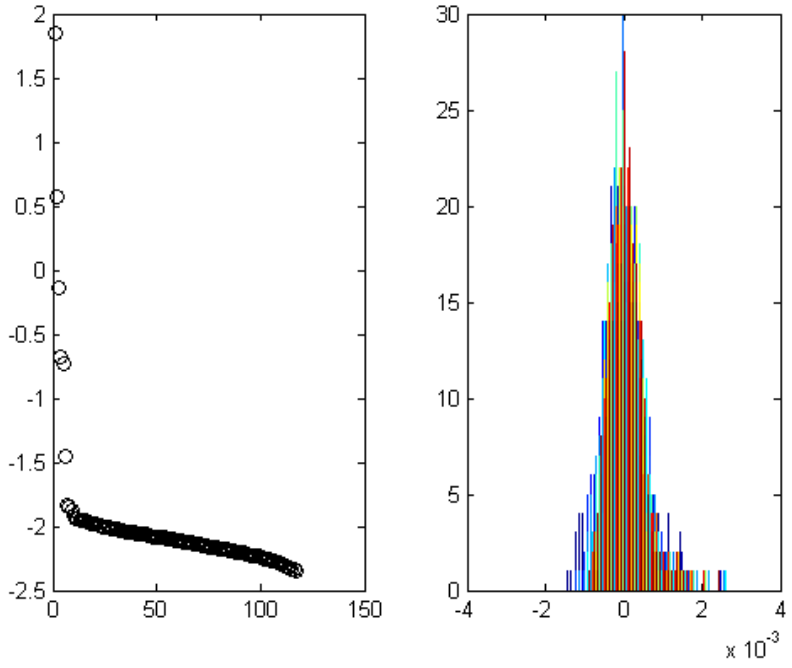

Figure S8: **Left:** Semilog plot of singular values. **Right:** Histogram of residuals illustrating Gaussian distribution of remaining signal.

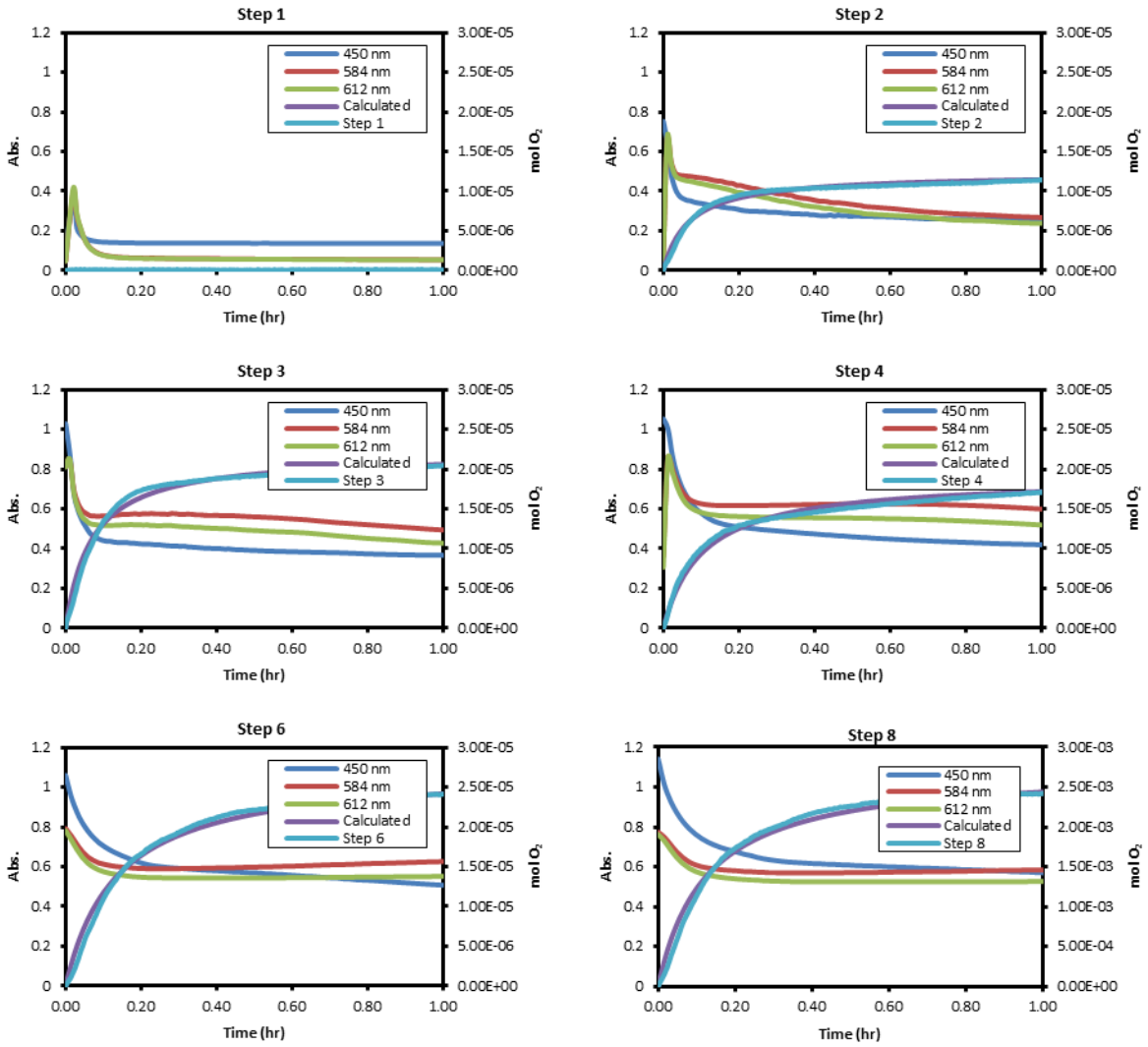

Figure S9: Absorbtion, experimentally observed, and least squares fit of oxygen traces from previously described experiment featuring regular sequential additions of cerium(IV) to an aqueous solution of **4a**.

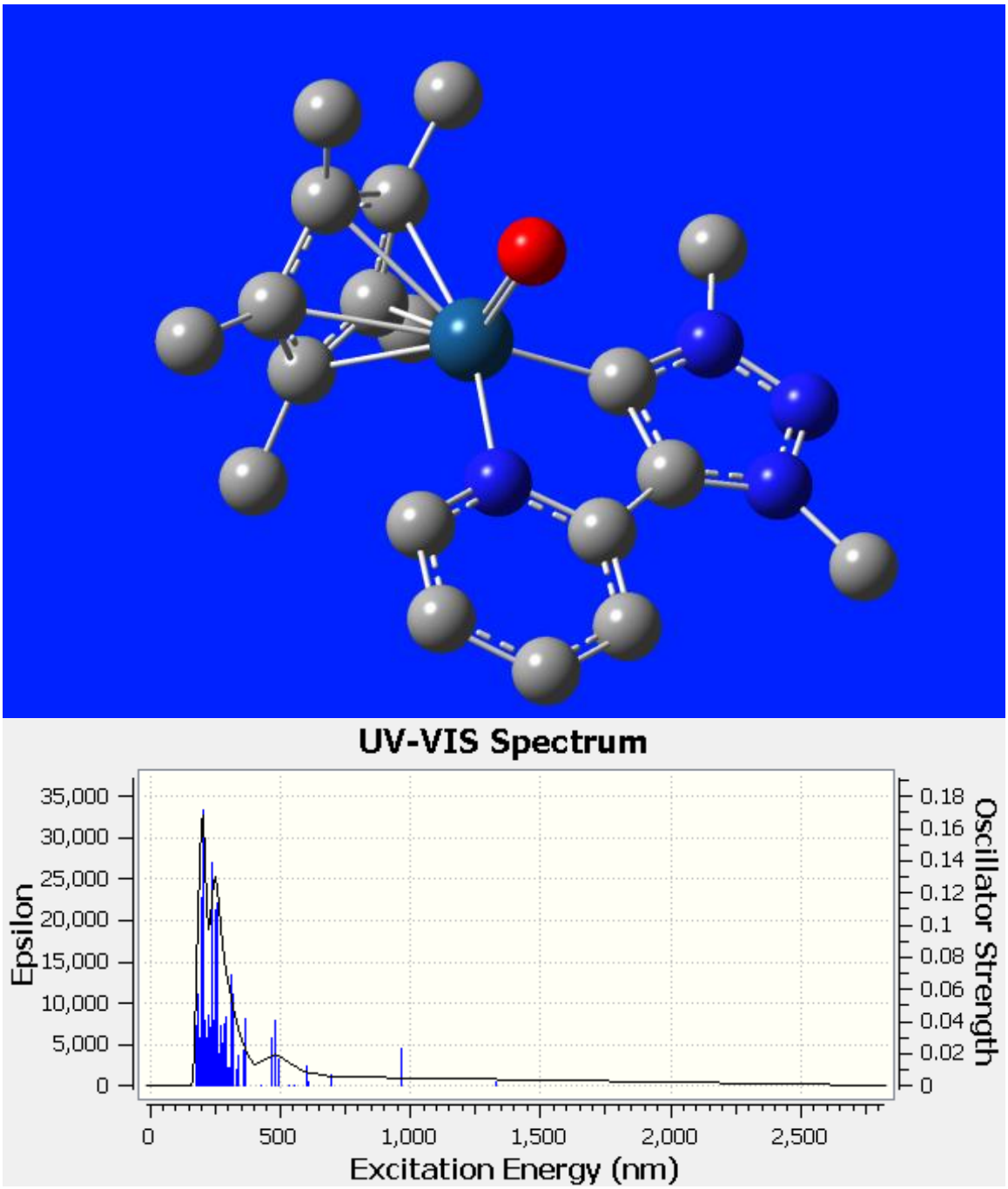

Figure S10a: Compound 4c Ir(III)=O (singlet)

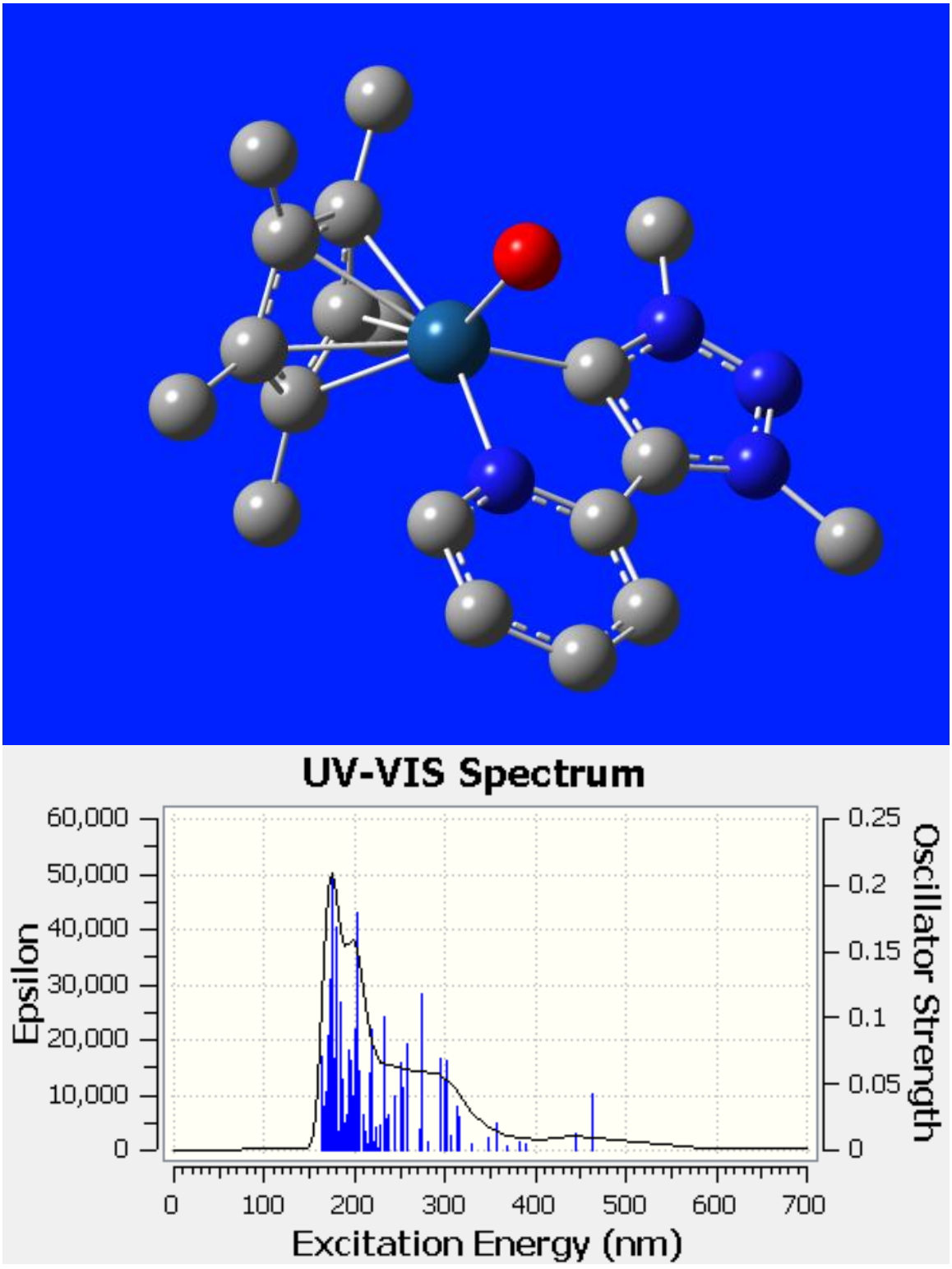

Figure S10b: Compound 4c Ir(III)-OH (singlet)

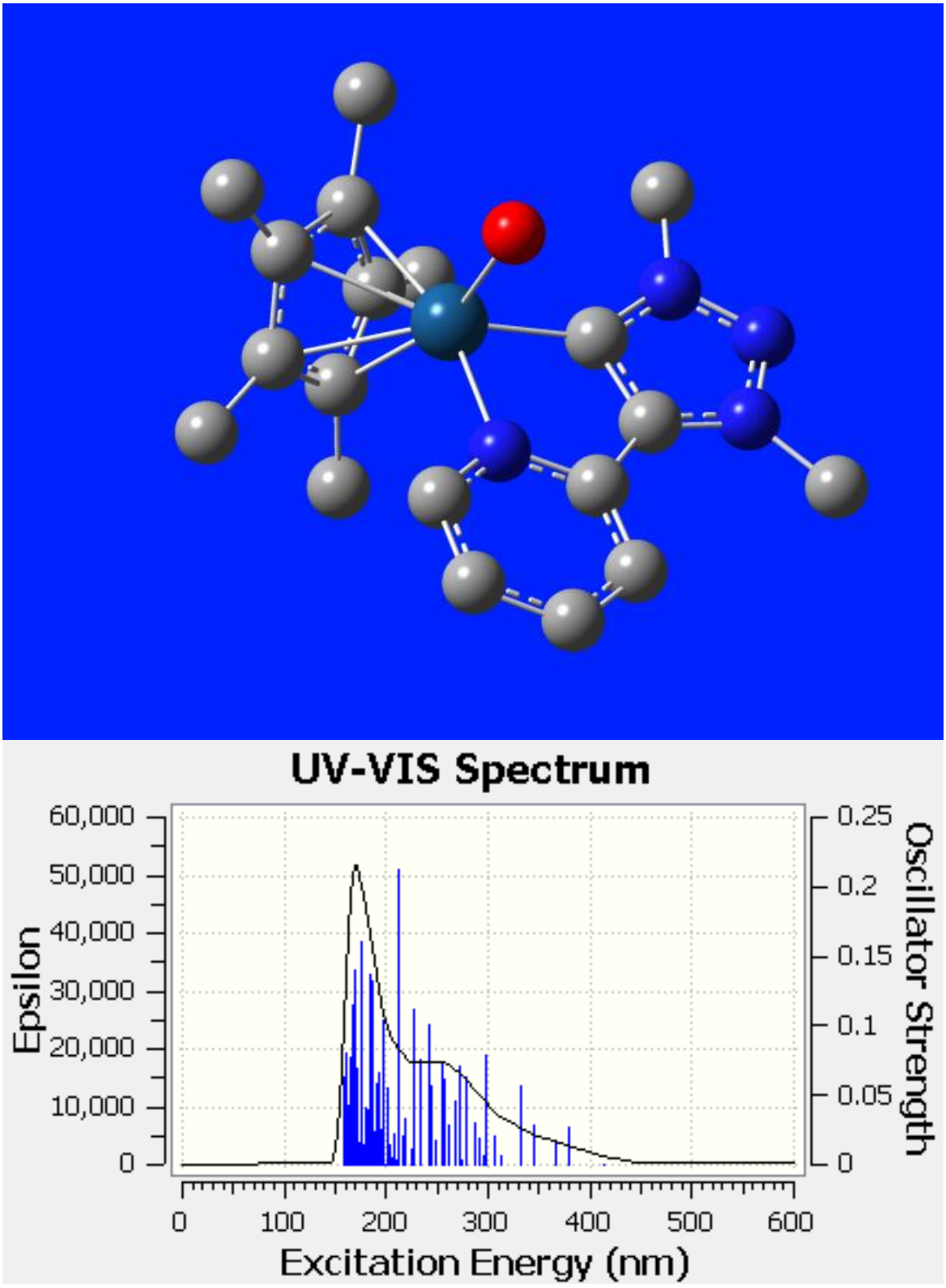

Figure S10c: Compound 4c Ir(III)-OH_2 (singlet)

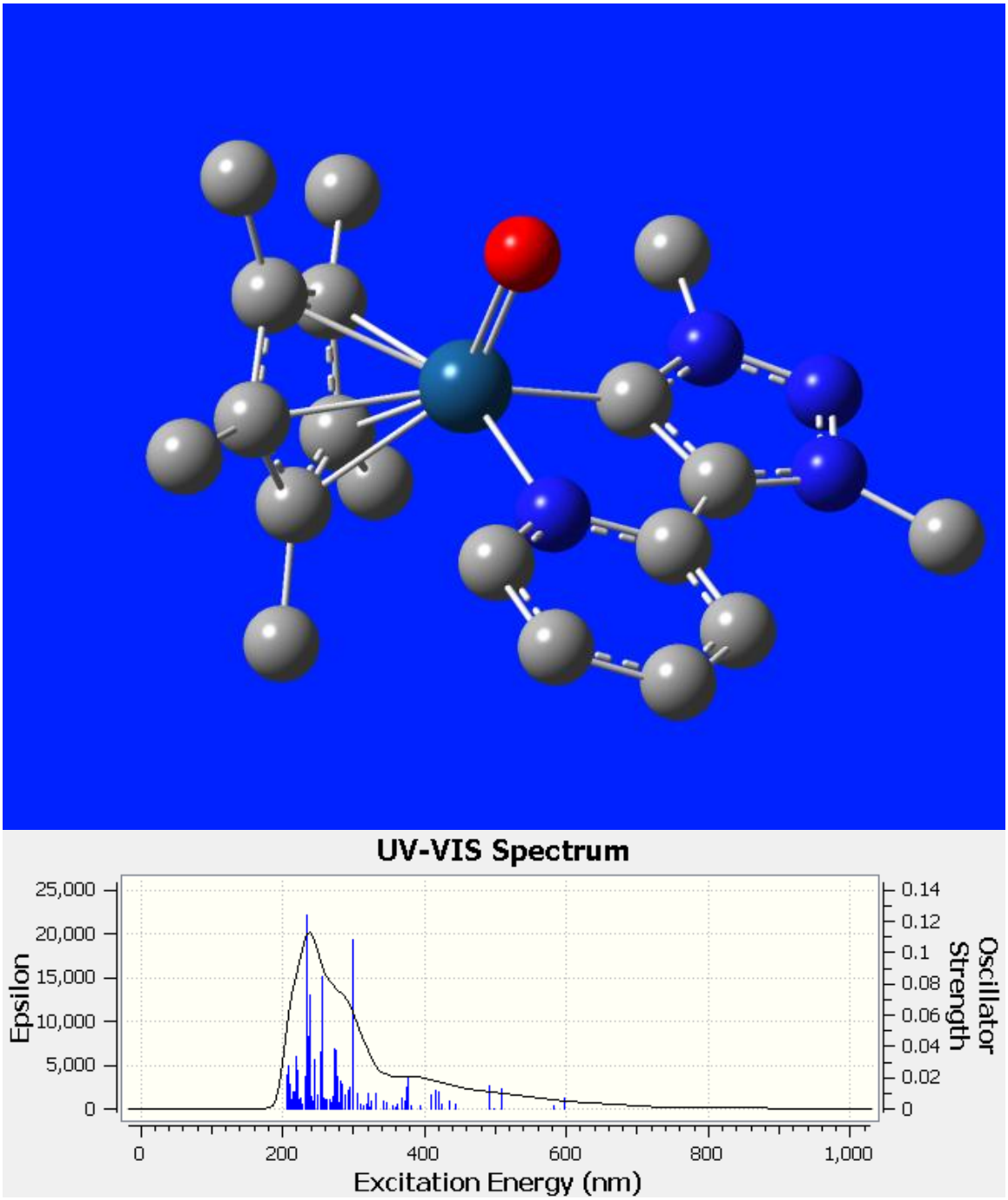

Figure S10d: Compound 4c Ir(IV)=O (doublet)

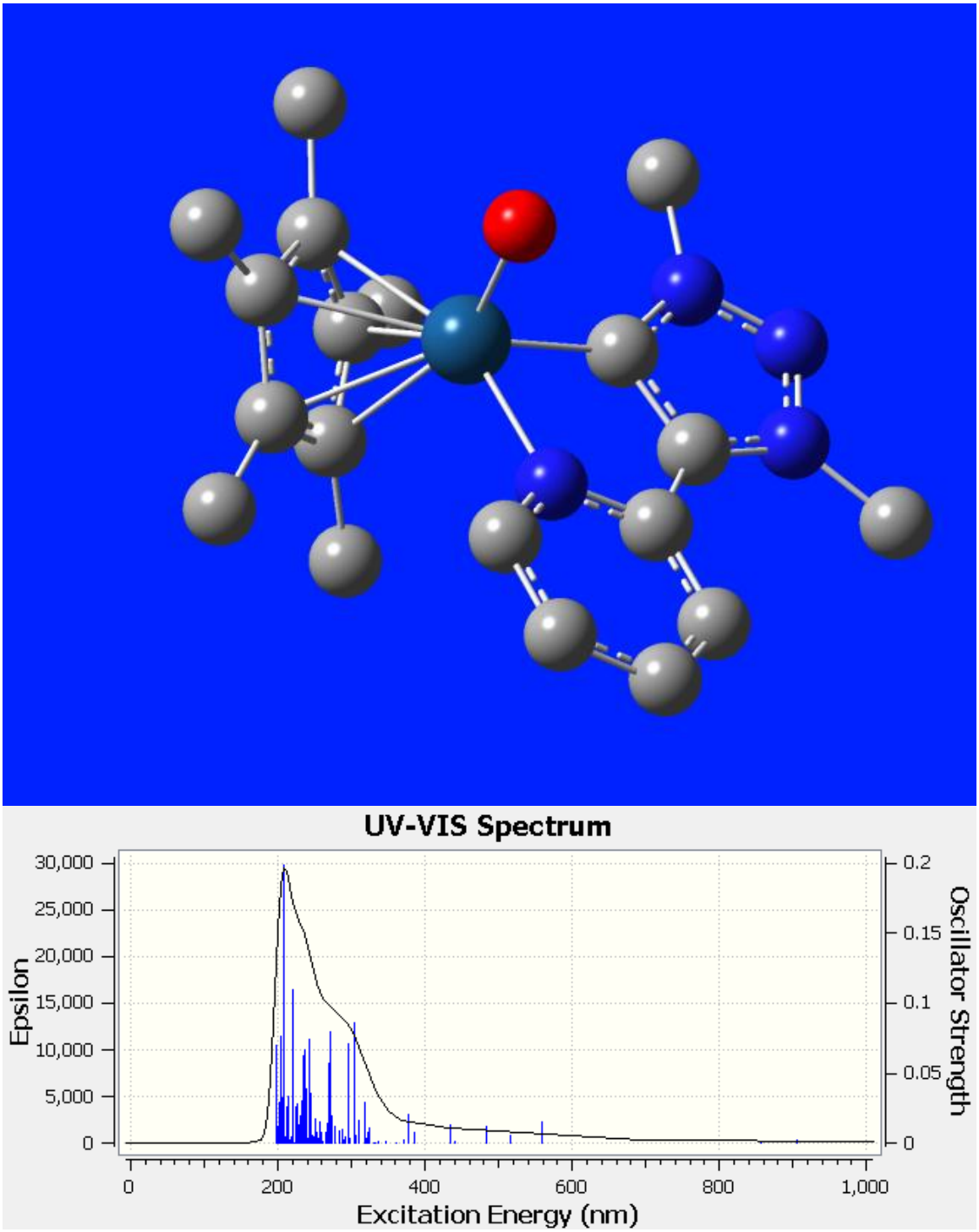

Figure S10e: Compound 4c Ir(IV)-OH (doublet)

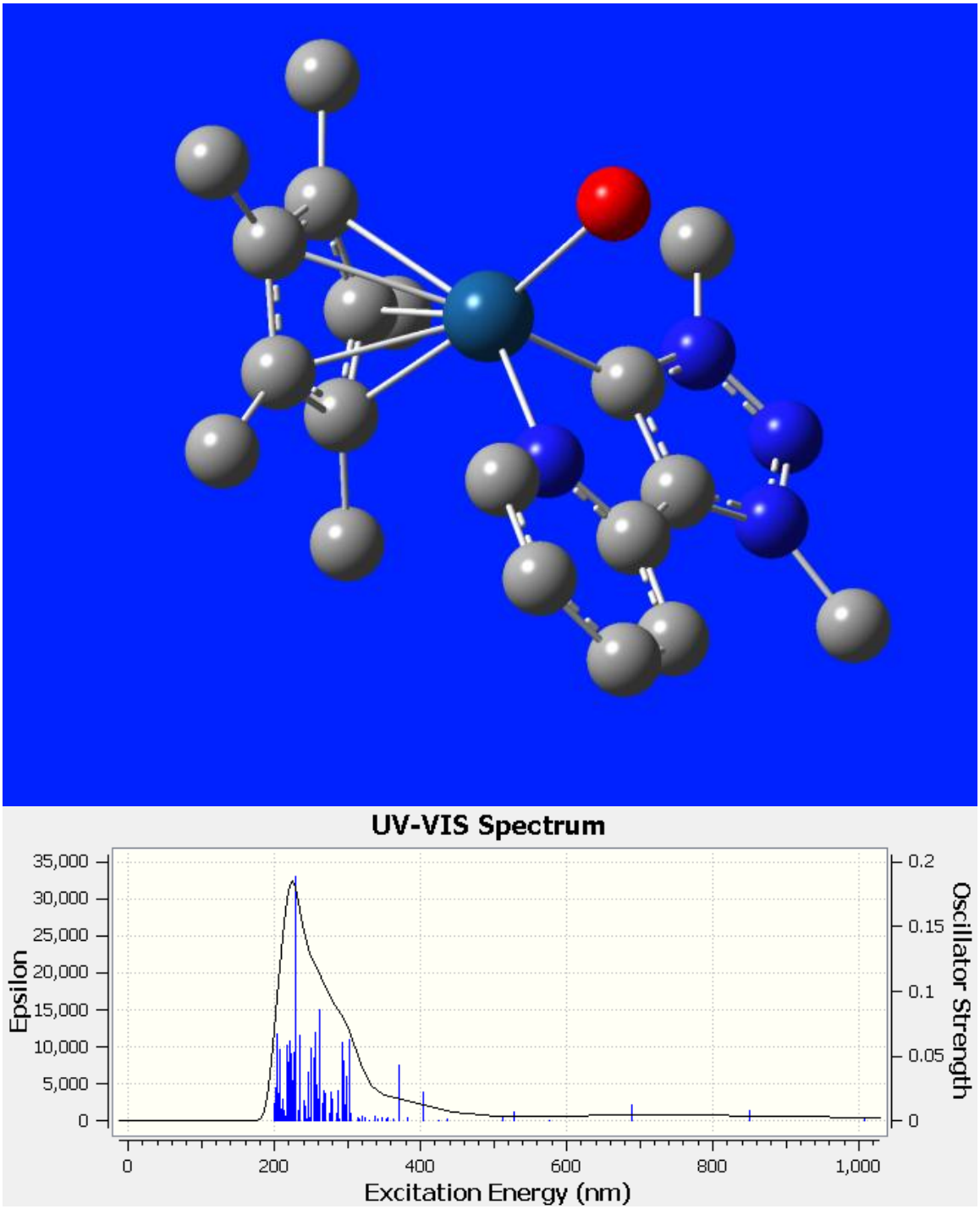

Figure S10f: Compound 4c Ir(IV)-OH_2 (doublet)

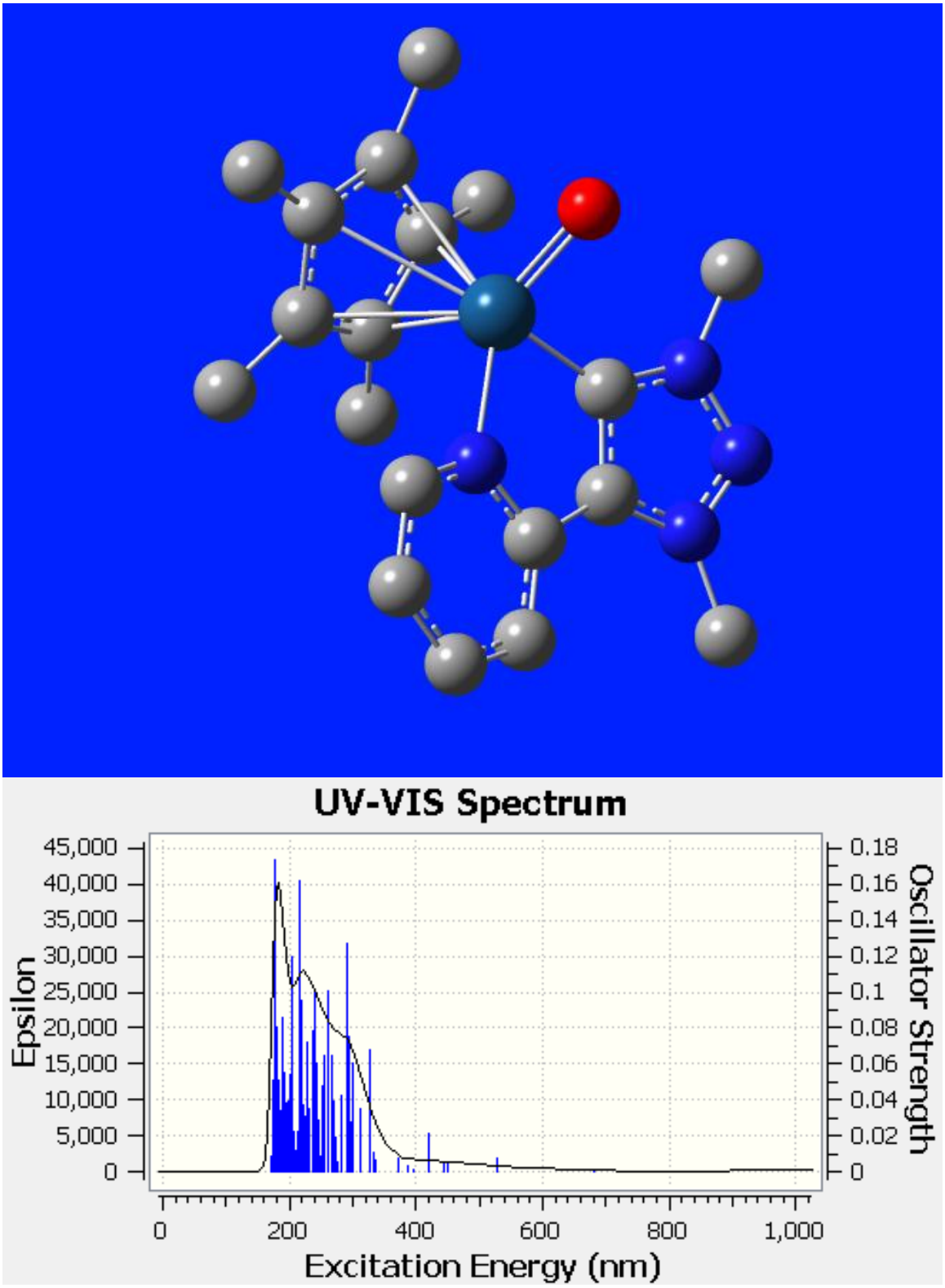

Figure S10g: Compound 4c Ir(V)=O (singlet)

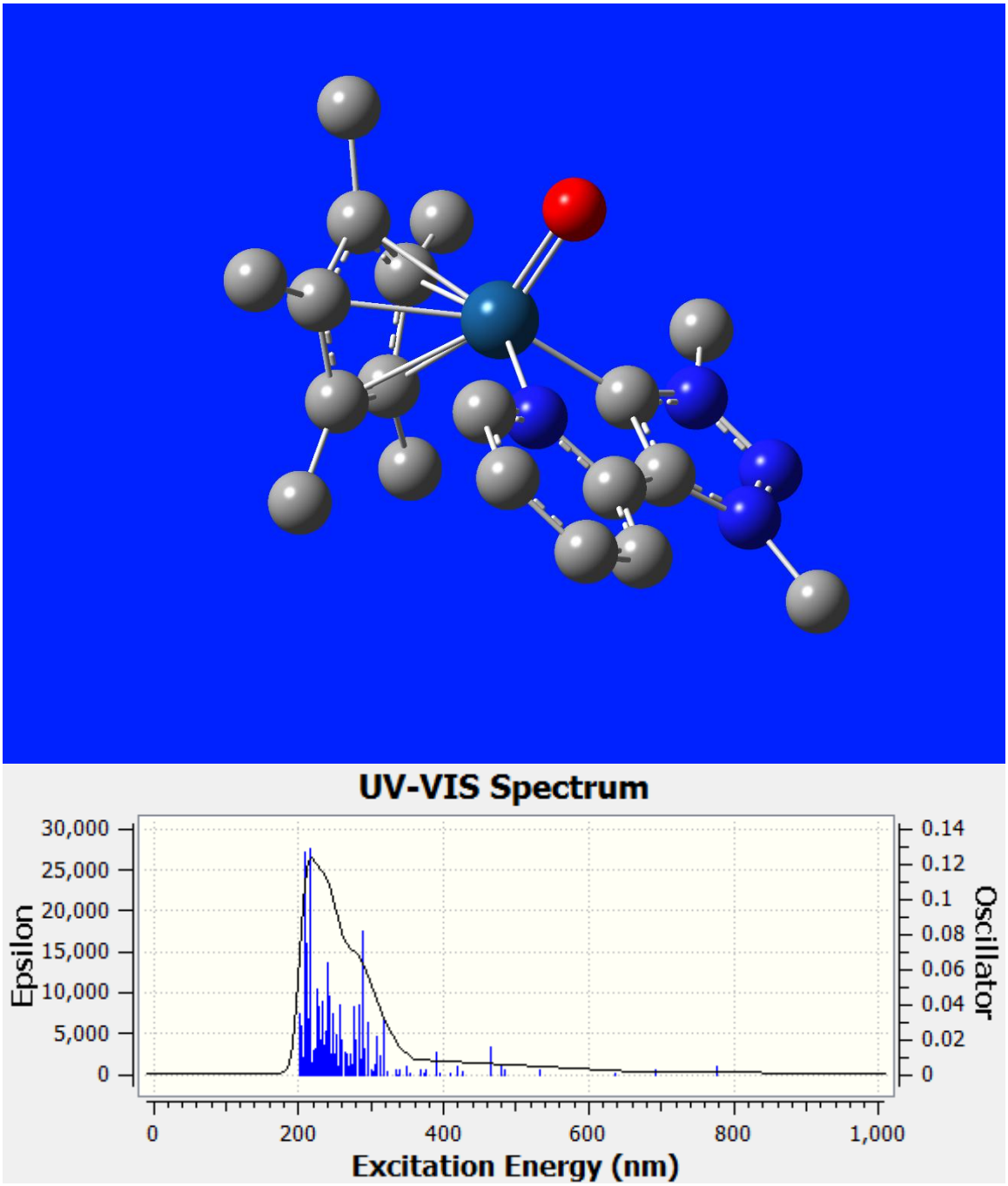

Figure S10h: Compound 4c Ir(V)=O (triplet)

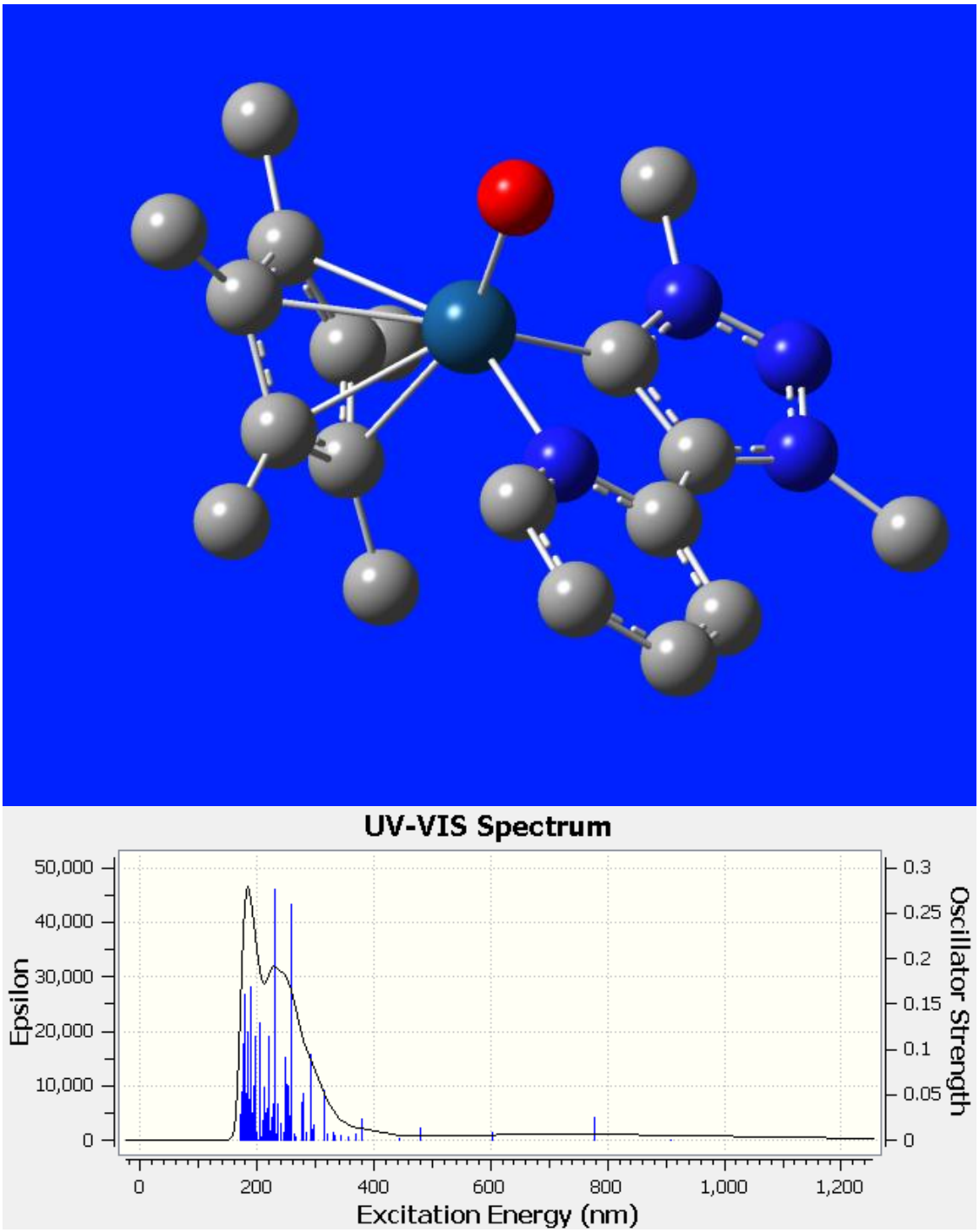

Figure S10i: Compound 4c Ir(V)-OH (singlet)

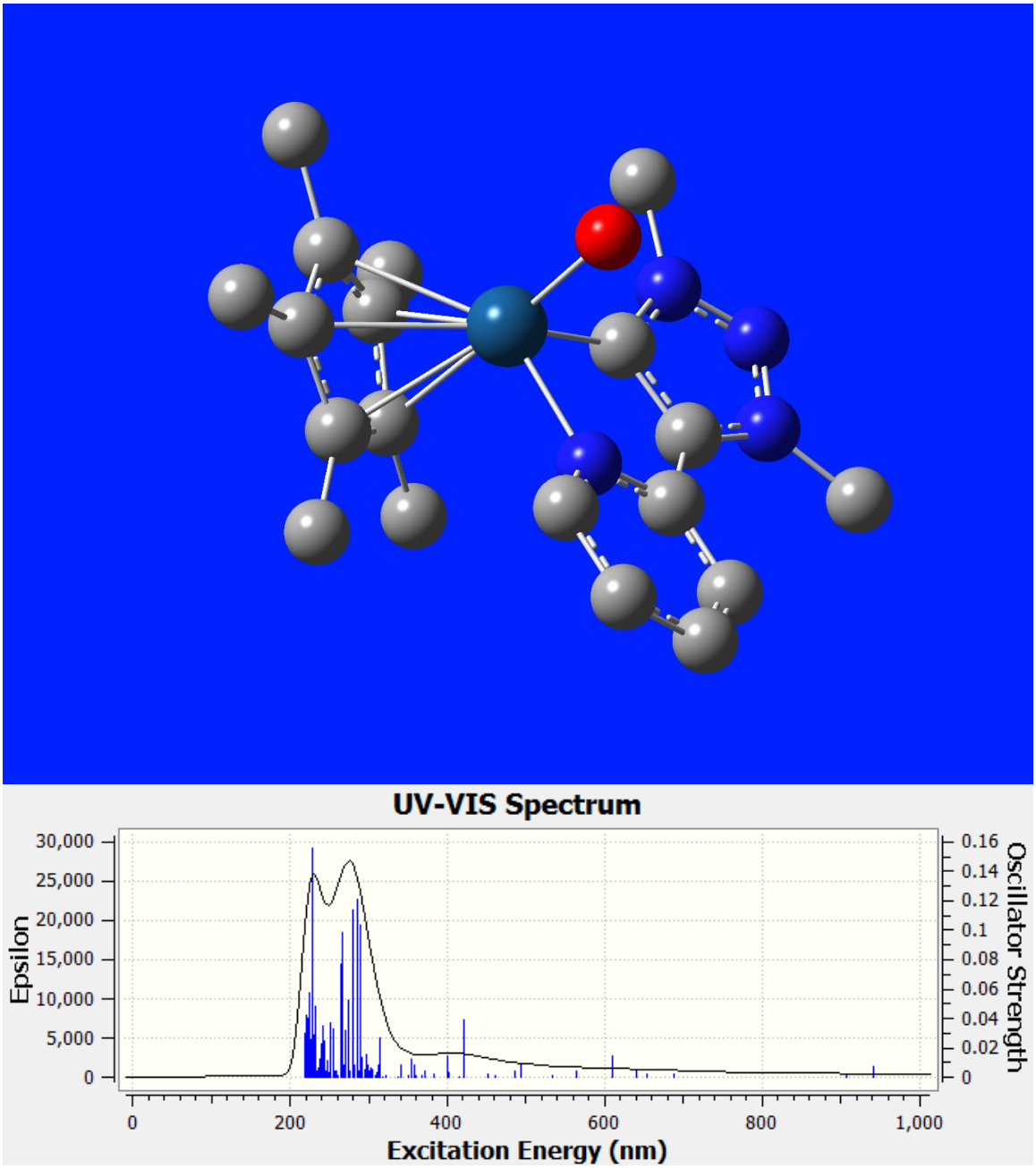

Figure S10j: Compound 4c Ir(V)-OH (triplet)

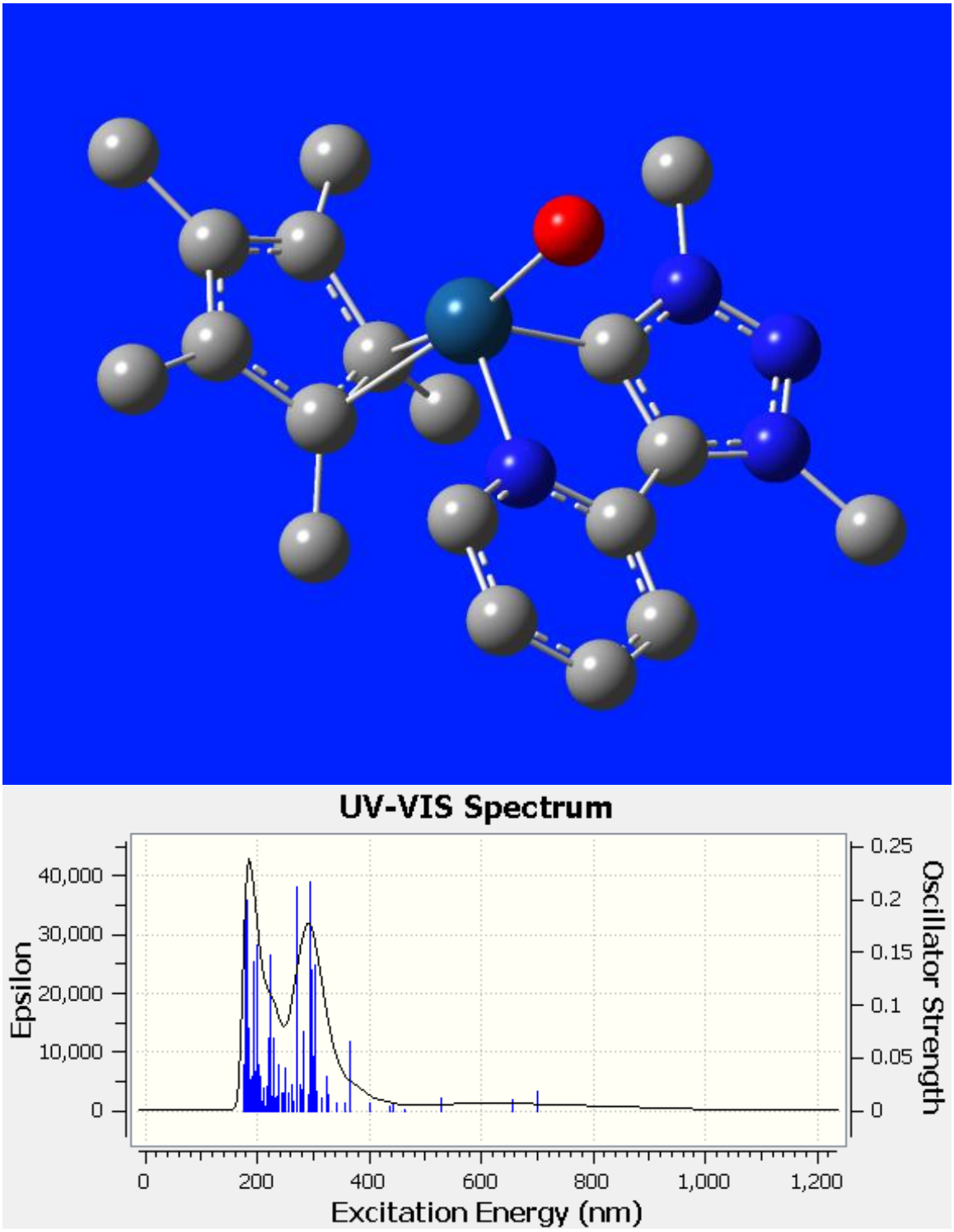

Figure S10k: Compound 4c Ir(V)-OH_2 (singlet)

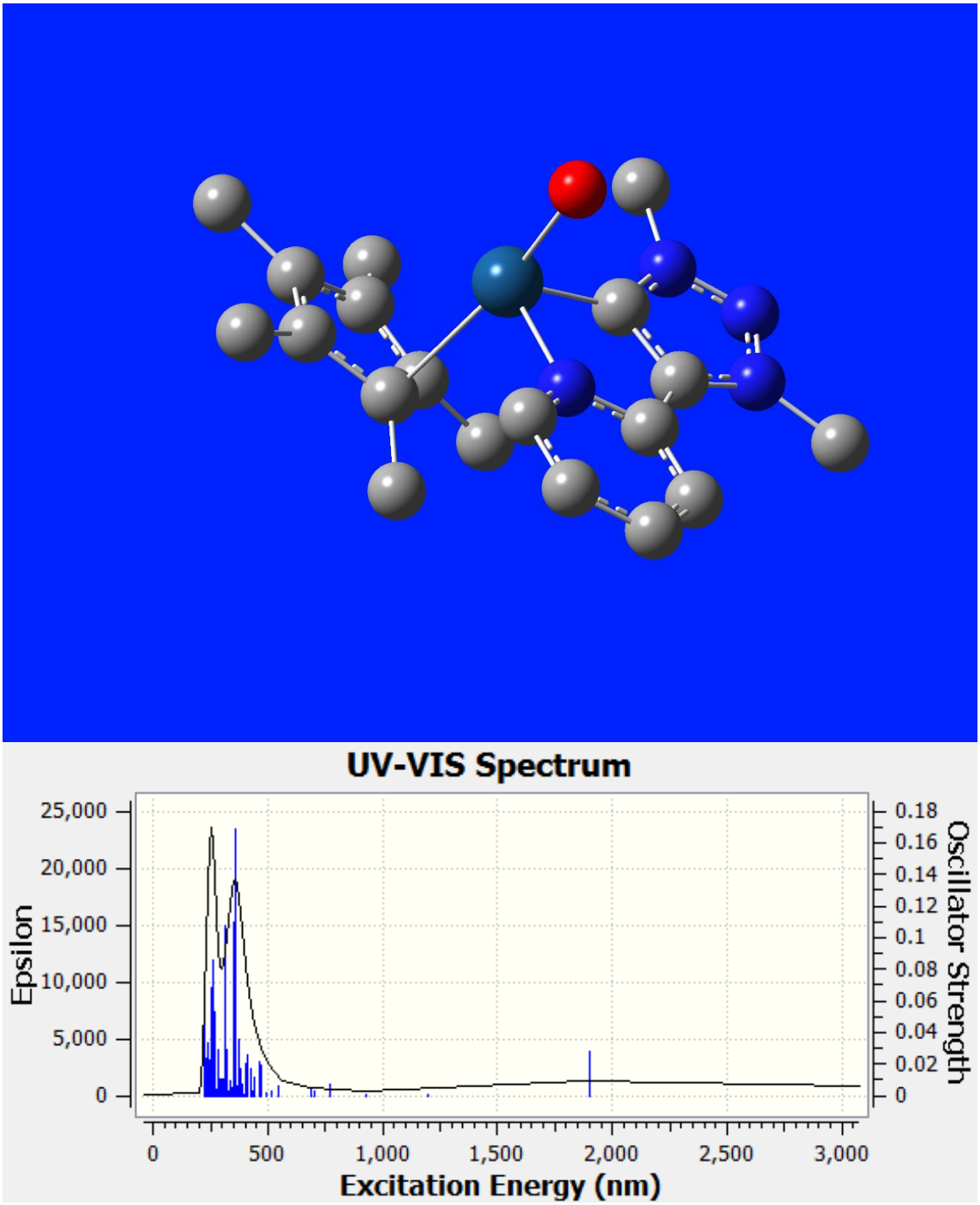

Figure S10l: Compound 4c Ir(V)-OH_2 (triplet)

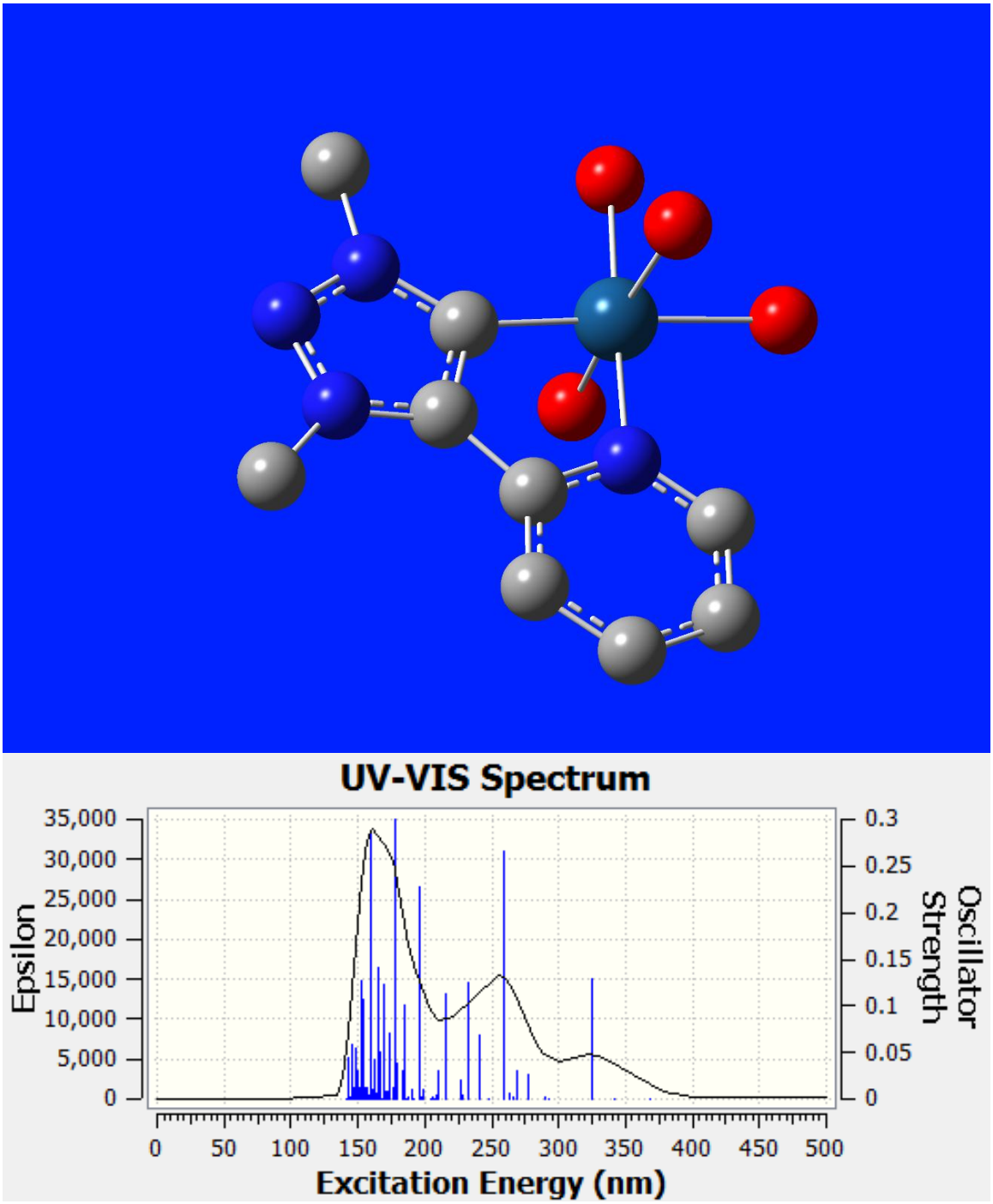

Figure S10m: Compound 4c (sans Cp*) Ir(III) $(OH_2)_4$ (singlet)

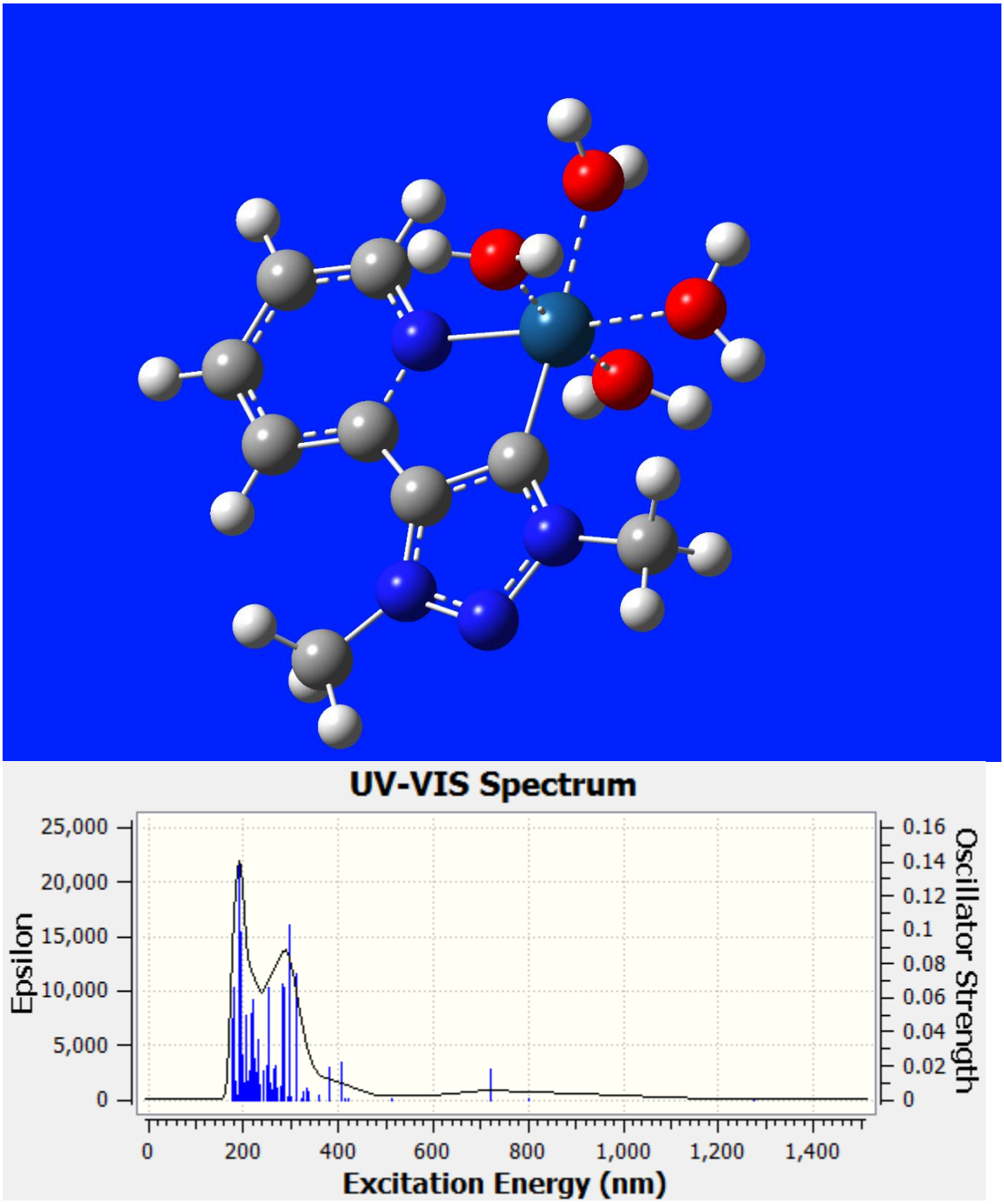

Figure S10n: Compound 4c (sans Cp*) Ir(III) $(OH_2)_4$ (triplet)

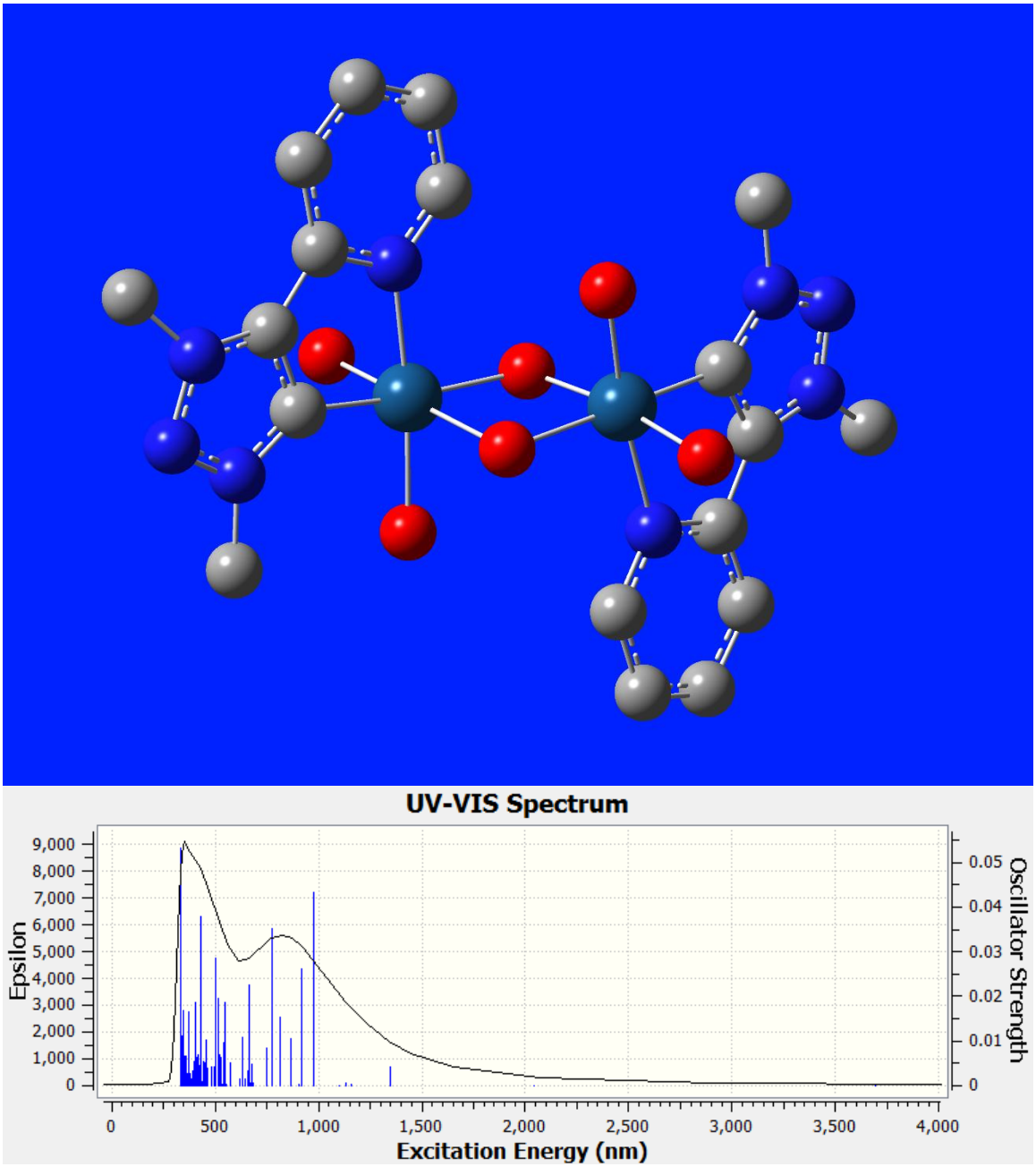

Figure S10o: 4c Dimer: Ir(3,3) A 2 OH B 2 OH (triplet)

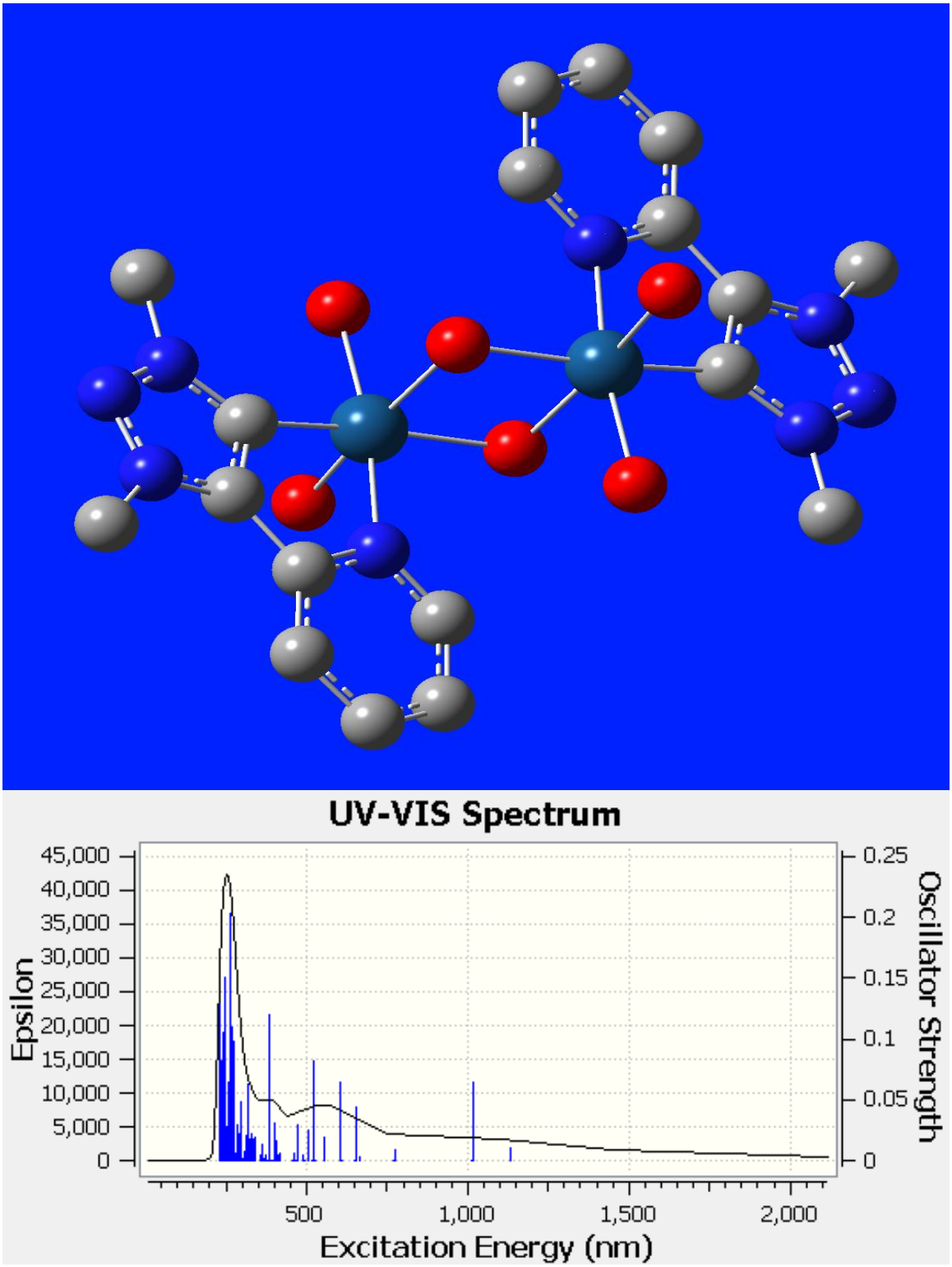

Figure S10p: 4c Dimer: Ir(3,3) A 2 OH B 2 OH (singlet)

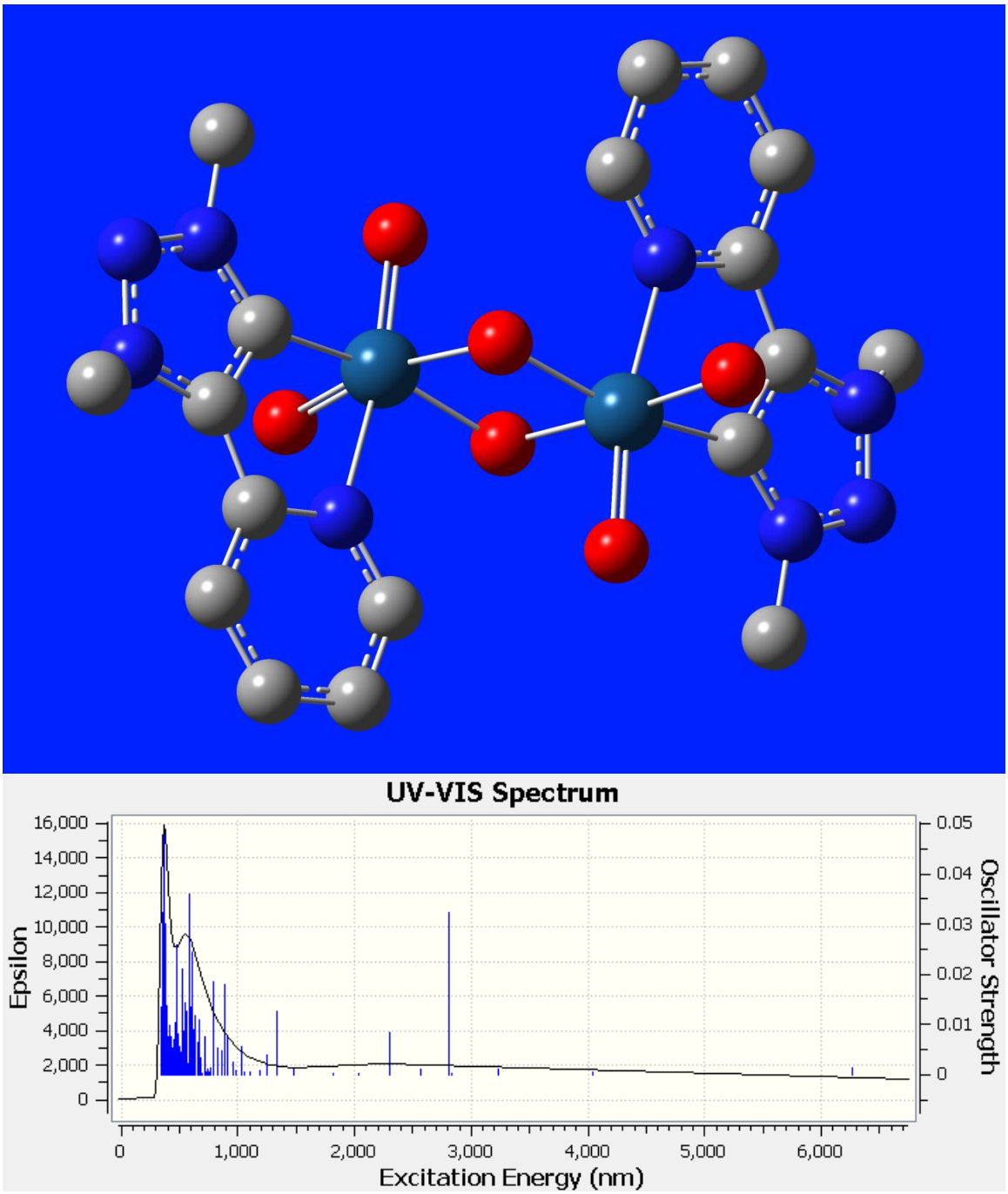

Figure S10q: 4c Dimer: Ir (3,4) A ax OH eq O B 2 O (doublet)

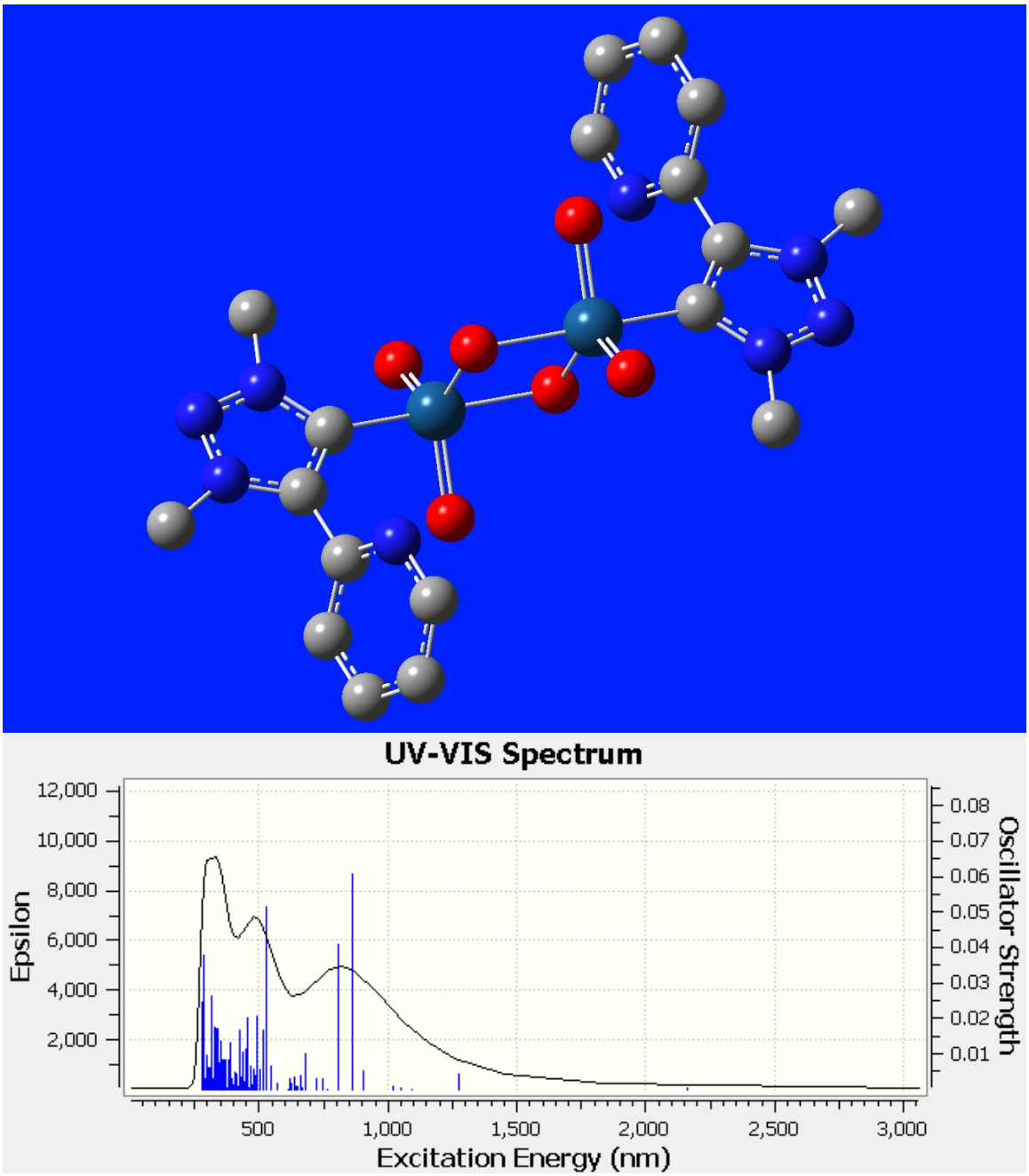

Figure S10r: 4c Dimer: Ir(5, 5) A 2 O B 2 O (singlet)

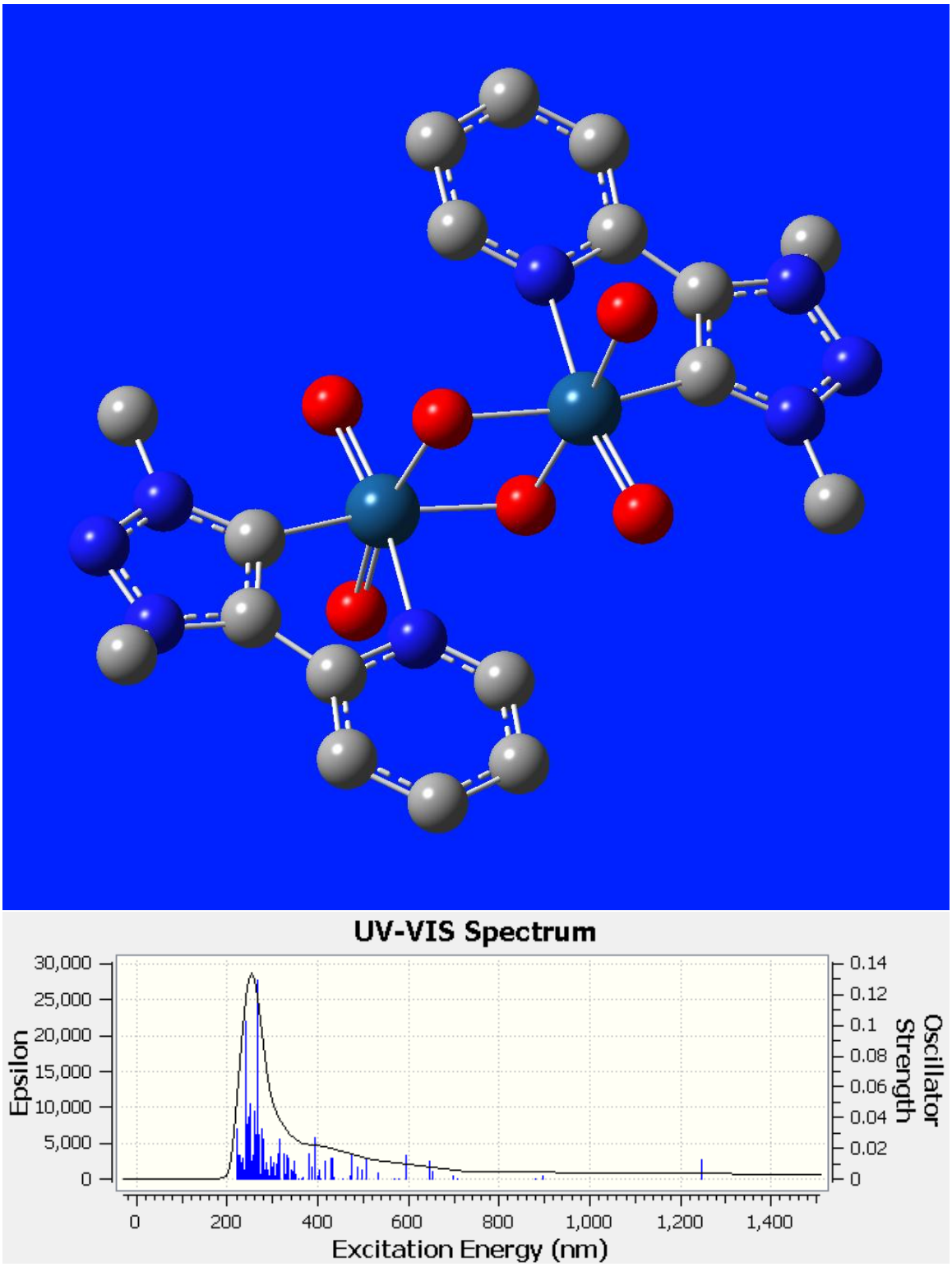

Figure S10s: 4c Dimer: Ir(5,5) A ax OH eq O B 2 O (singlet)

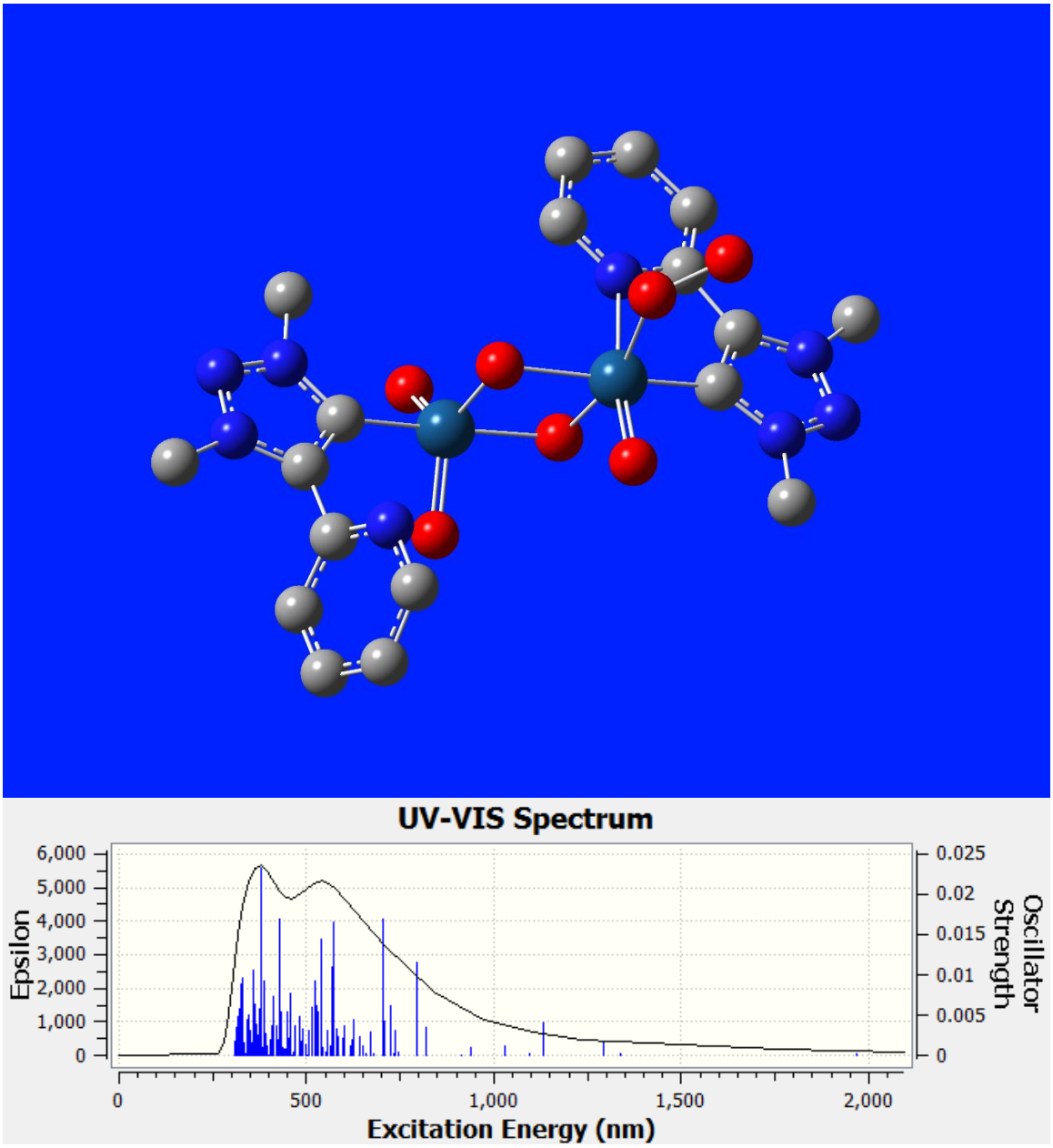

Figure S10t: 4c Dimer: Ir(5,5) A ax OOH eq O B 2 O (singlet)

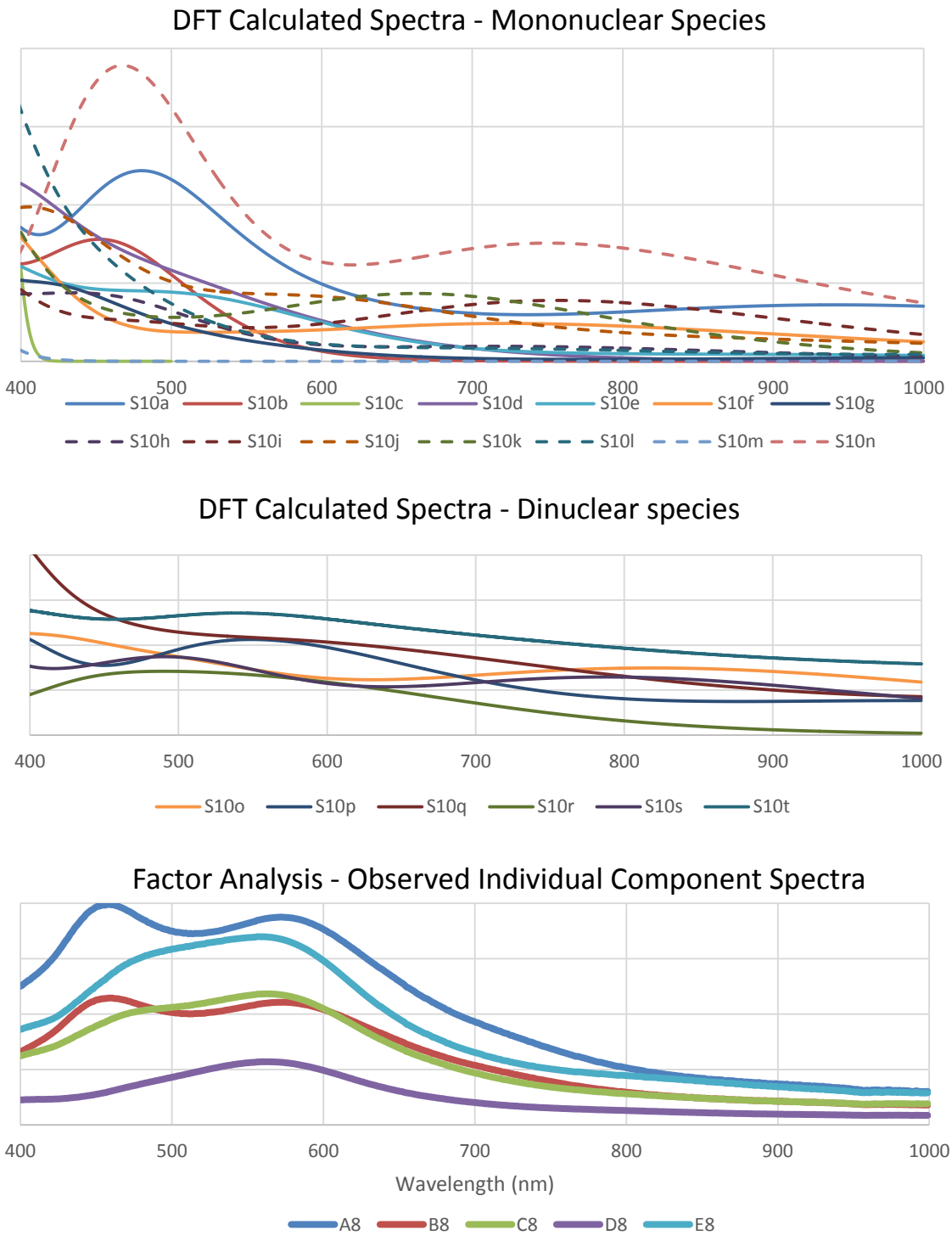

Figure S11: Comparison of calculated spectra of (Cp*)-containing mononuclear and dinuclear species resulting from various oxidation states and protonation with the spectra obtained by factor analysis.

DLS measurements

Dynamic light scattering (Malvern Nano ZS) were performed at low and medium CAN:**4a** ratios. In a first set of experiments, the stepwise addition of CAN mimicking the conditions of Fig. 6 was reproduced and monitored by DLS. The complex at pH 0 does not indicate the presence of scattering particles larger in size than the long axis of an ellipsoid circumscribing the force field-reduced structure of **4a** (MM2 ca. 0.97 nm; Fig. S8). CAN was subsequently added in 20 equiv portions and measurements were performed immediately after addition, after 15 min (when O_2 evolution rates are high, see manuscript), and after 2 h (when O_2 evolution has essentially ceased). At this stage, another 20 equiv portion of CAN was added. The particle distribution is shown in Fig. S8–11.

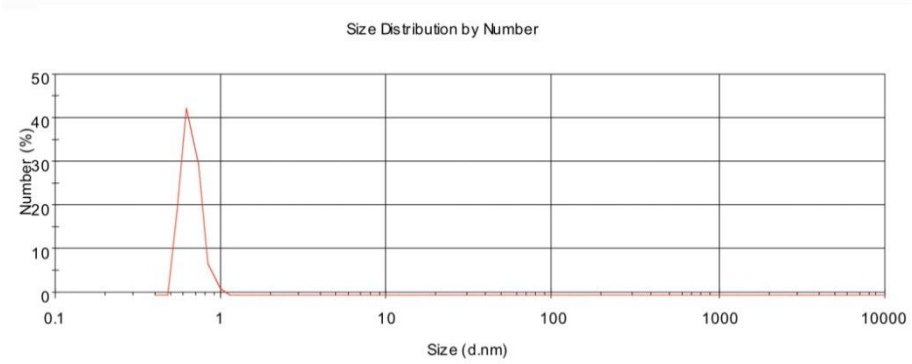

Fig. S12 DLS response of a solution of complex **4a** at pH 0 (5 mM, 1 M HNO_3).

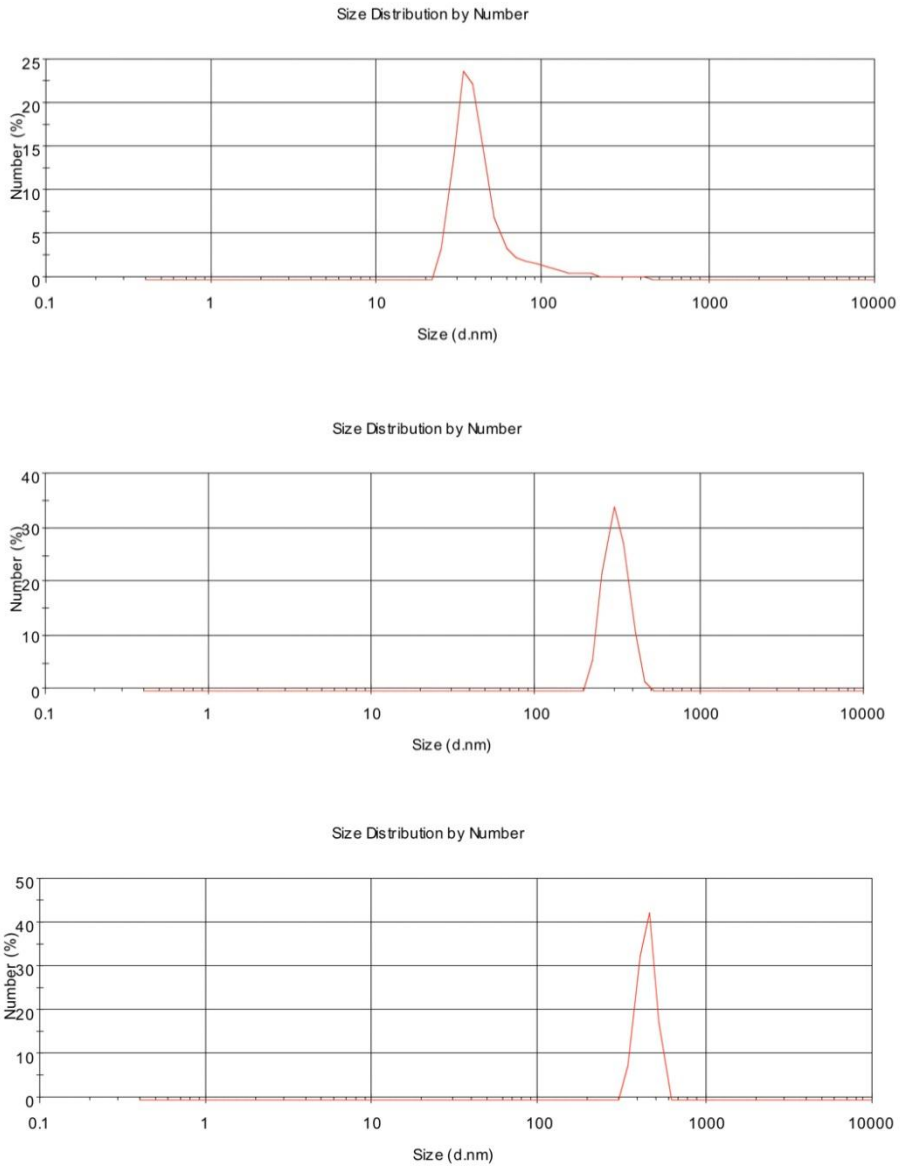

Fig S13 Addition of a first batch of CAN (20 equiv.), measured immediately after addition (top), 15 min after addition (middle) and 2 h after addition (bottom).

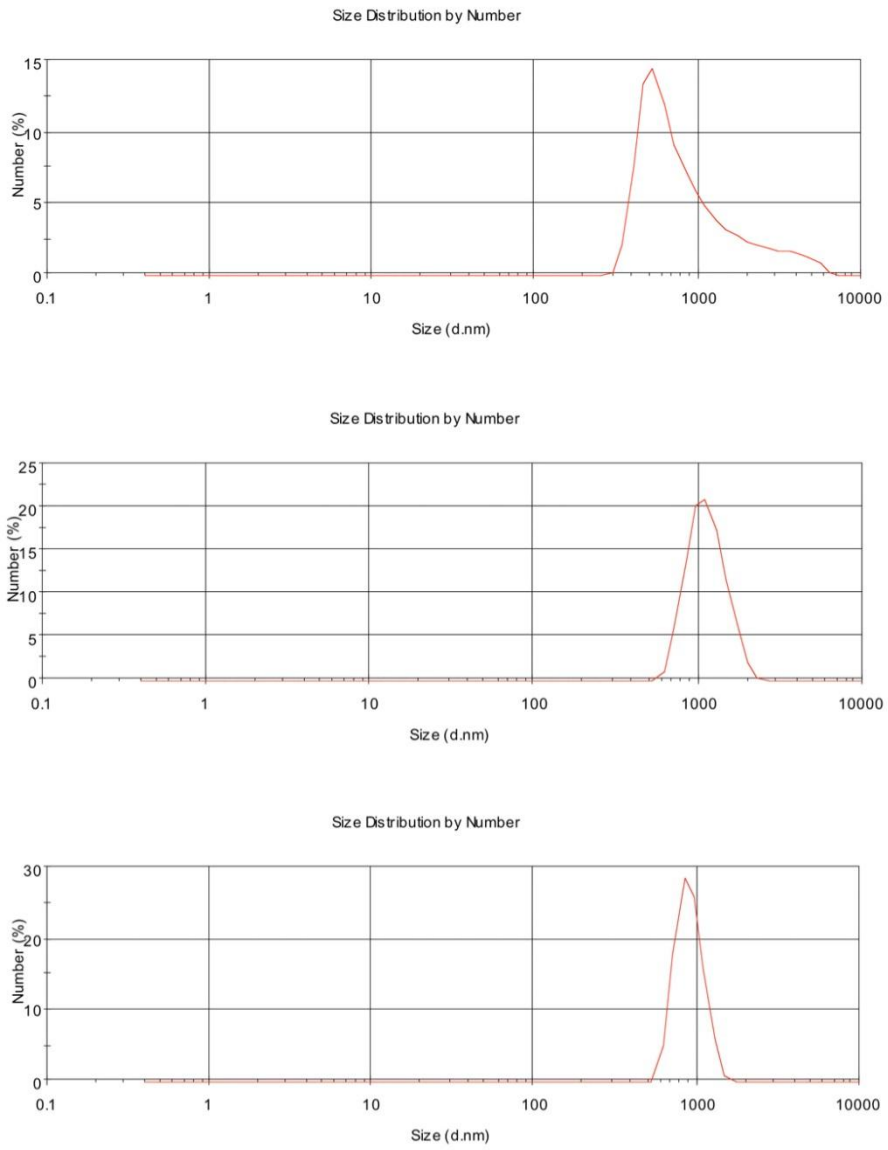

Fig S14 Addition of a third batch of CAN (60 equiv. total), measured immediately after addition (top), 15 min after addition (middle) and 2 h after addition (bottom).

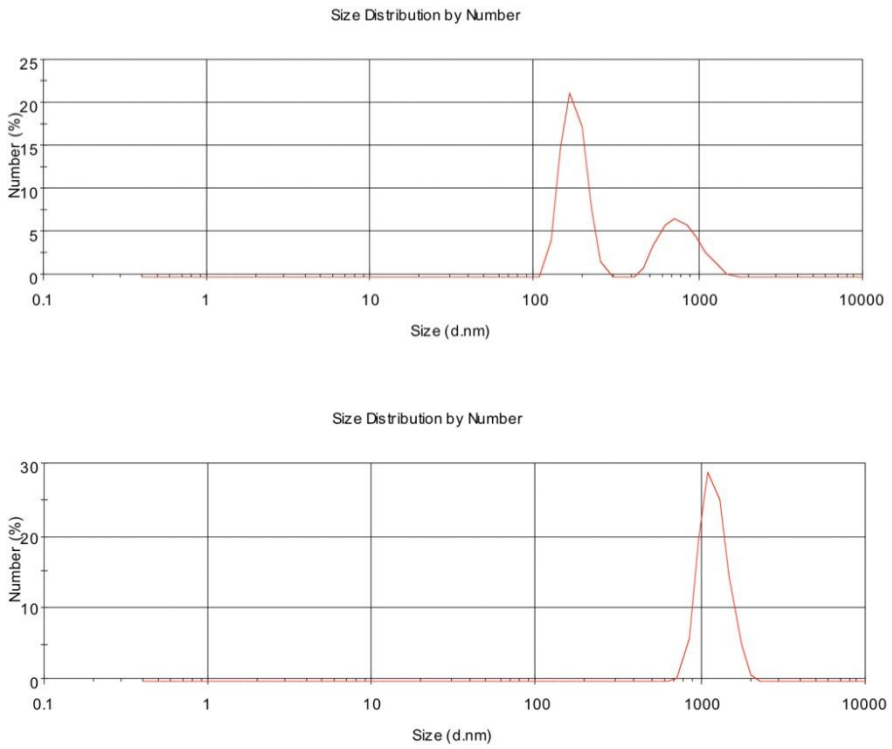

Fig S15 Addition of a fourth batch of CAN (80 equiv. total), measured immediately after addition (top) and 15 min after addition (bottom).

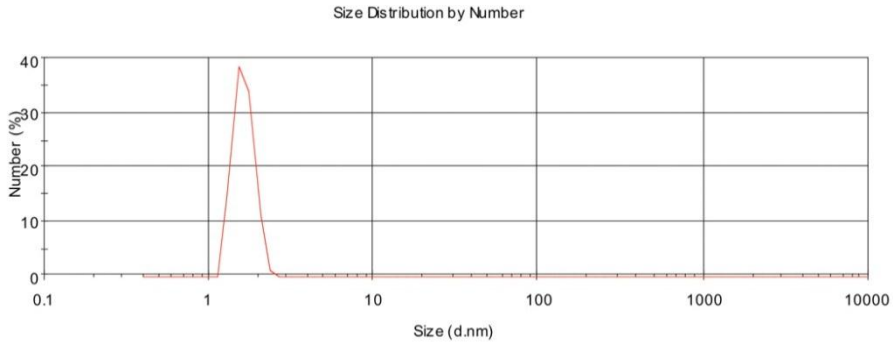

Fig S16 Addition of a gross excess CAN (600 equiv. total), measured 40 h after addition.

The scattering objects observed during the measurement appear to have a dynamic radius with their size varies rapidly (see eg the 200 nm signal after addition of the fourth batch of CAN, and the disappearance of this signal after 15 min; Fig. S5). Moreover, no particles were detected after prolonged standing of a solution treated with excess CAN (Fig. S12). This behavior is not commensurate with the formation of IrO_x particles as literature reports of iridium nanoparticles and nanoclusters are generally remarked for their persistence. No precipitate was observed after this reaction, thus excluding the aggregation of large particles. Moreover, the particle size is pressure dependent. They shrink to 60–80 nm upon applying a slight vacuum (600 mbar for 30 s) and expand again under normal pressure (Fig. S13). All these observations suggest that gas nucleation, likely O_2 owing to the headspace gas analysis, is responsible for the observed light scattering. No signs exist for persistent particles.

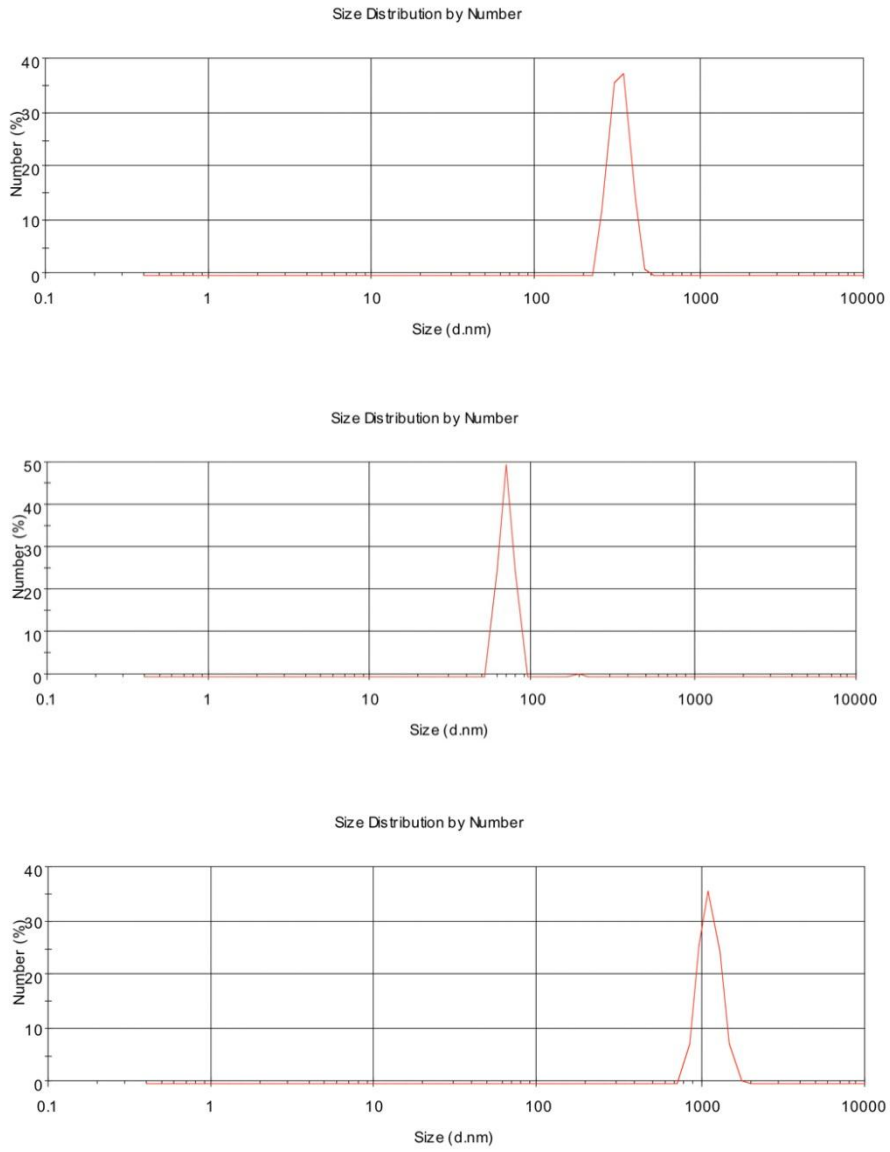

Fig. S17 Addition of a excess CAN (600 equiv. total) to a fresh solution of **4a** in 1 M HNO_3 measured 22 h after addition of CAN (top), after applying a vacuum (600 mbar for 30 s; middle), and after standing under atmospheric pressure for 10 min (bottom).

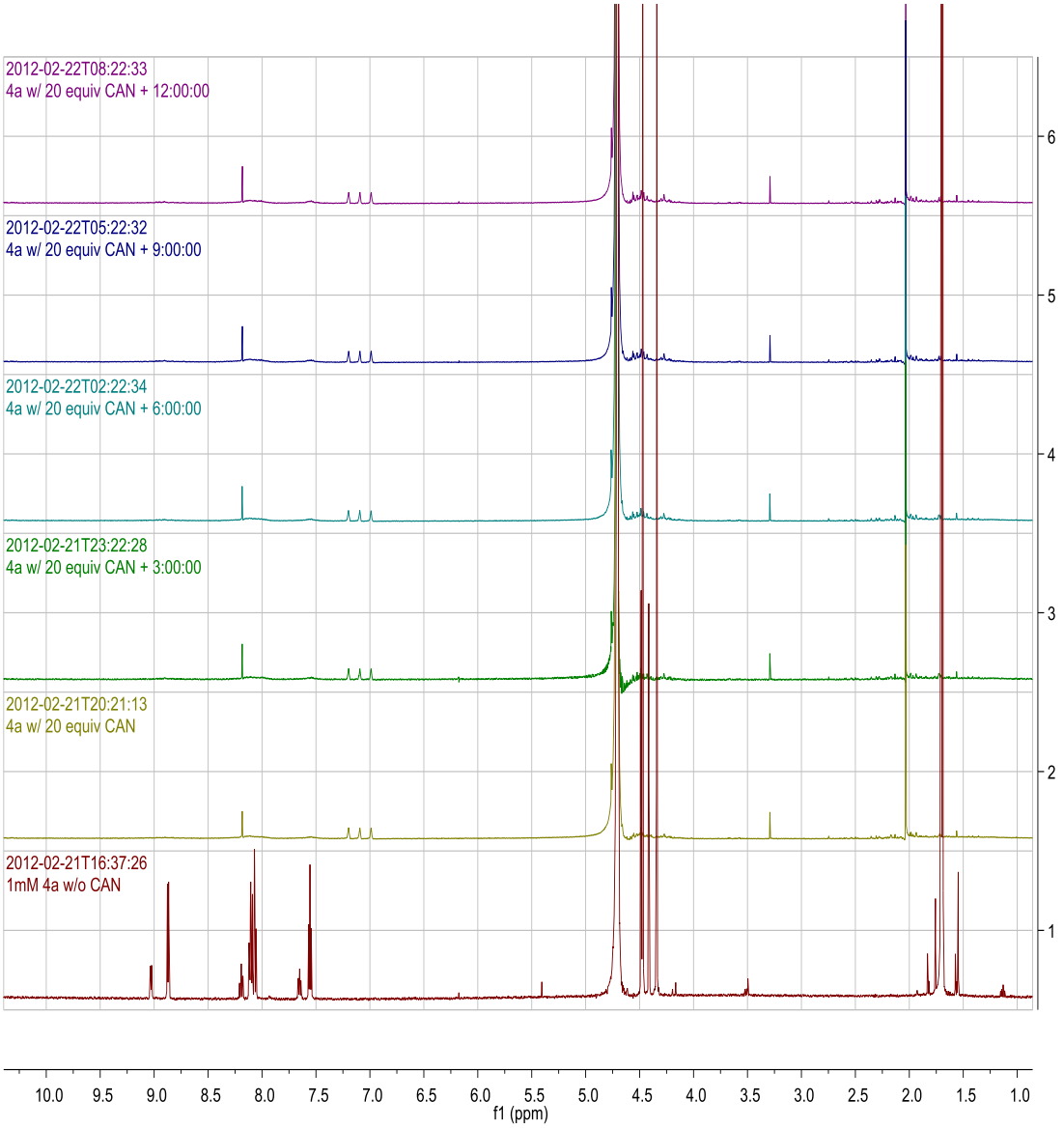

Figure S18: Addition of 20 equiv. of ceric ammonium nitrate to **4a** in 1N HNO_3 buffered D_2O with subsequent monitoring over 12 hours. The spectrum of **4a** before addition of CAN (bottom trace in red) shows two species as a consequence of the equilibrium with the corresponding aquo complex akin to **4c**.

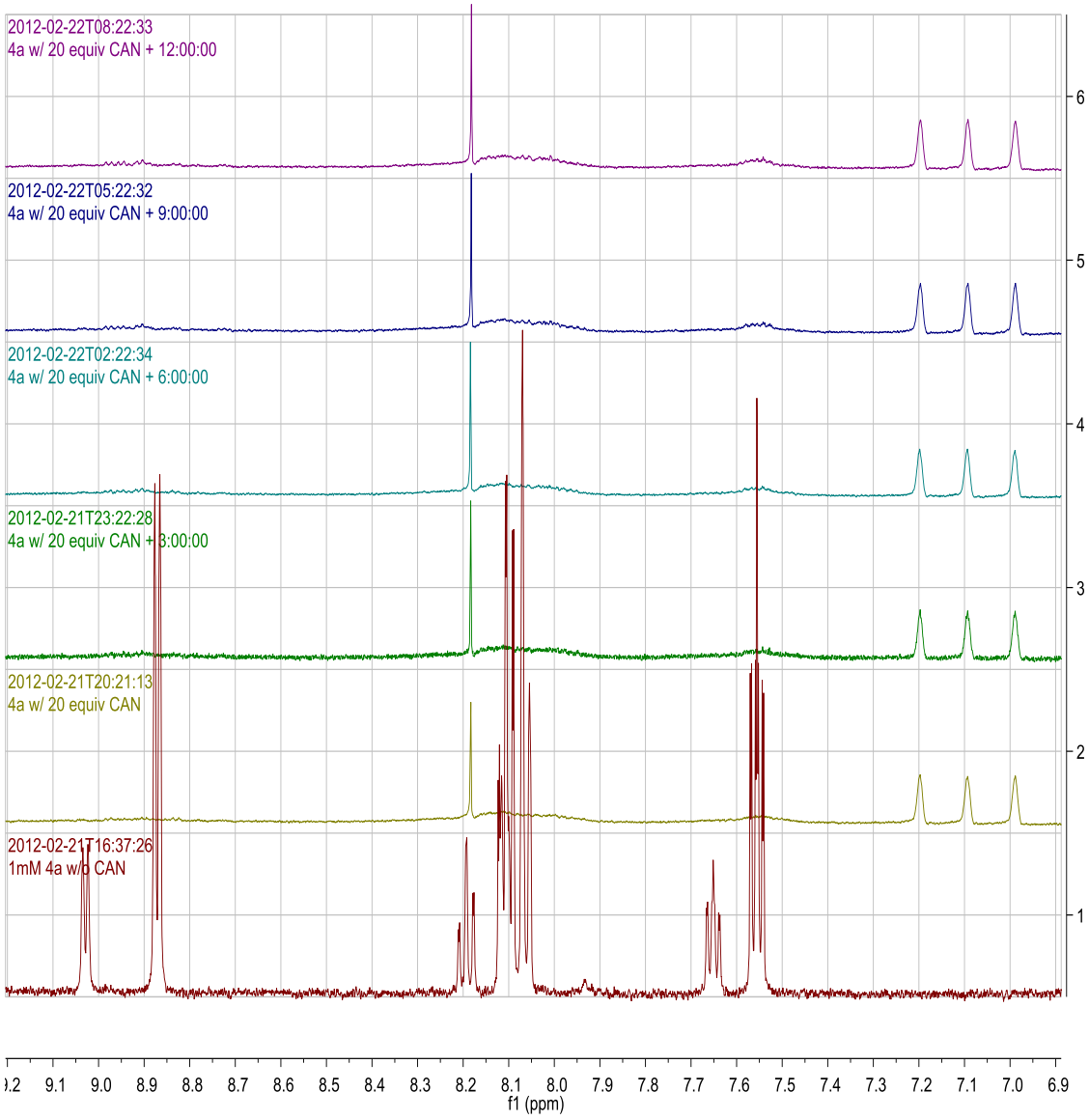

Figure S19: Expansion illustrating broad NMR signals suggesting a paramagnetic Ir species.

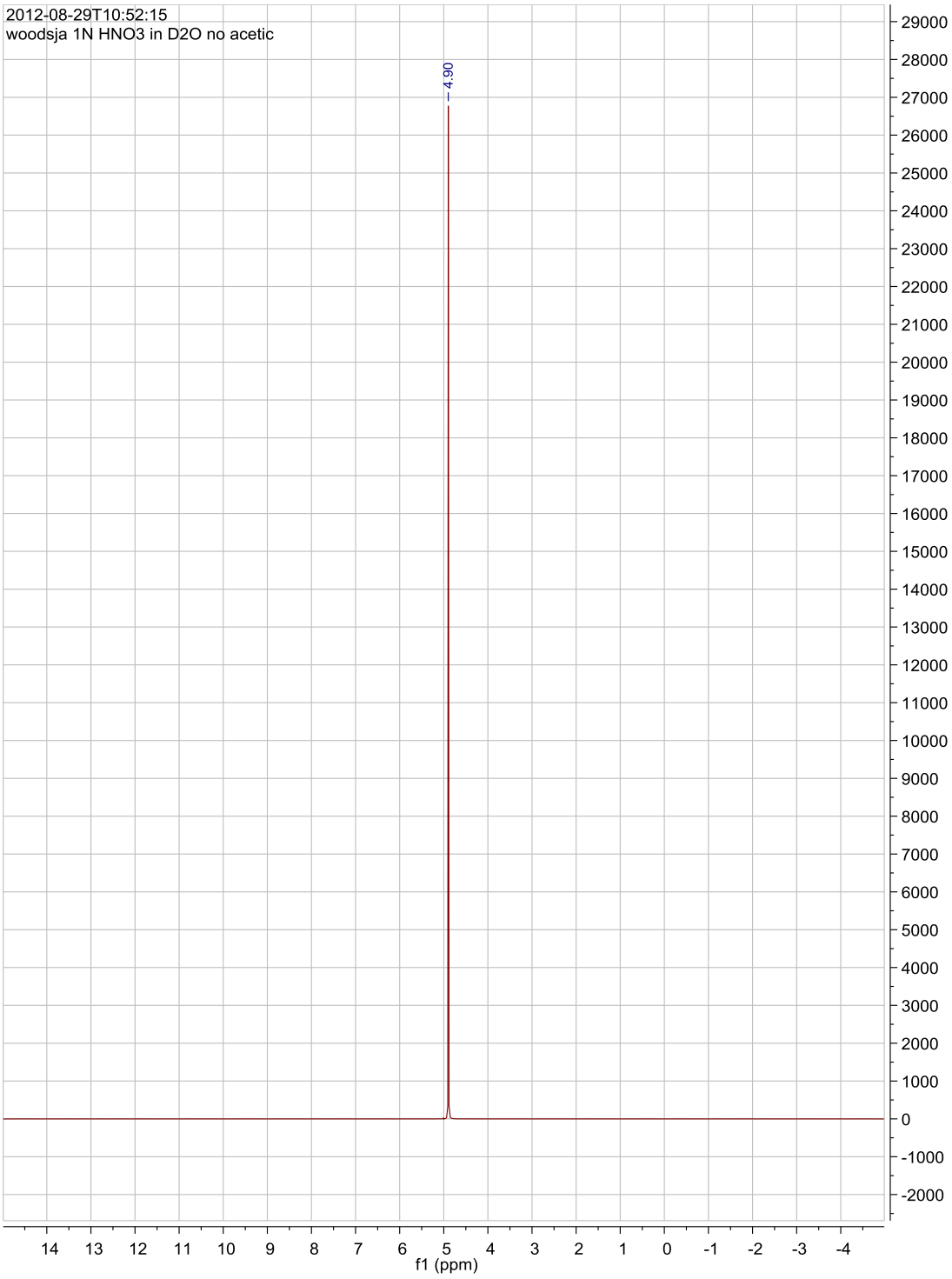

Figure S20: NMR spectrum of neat 1N HNO_3.in D_2O.

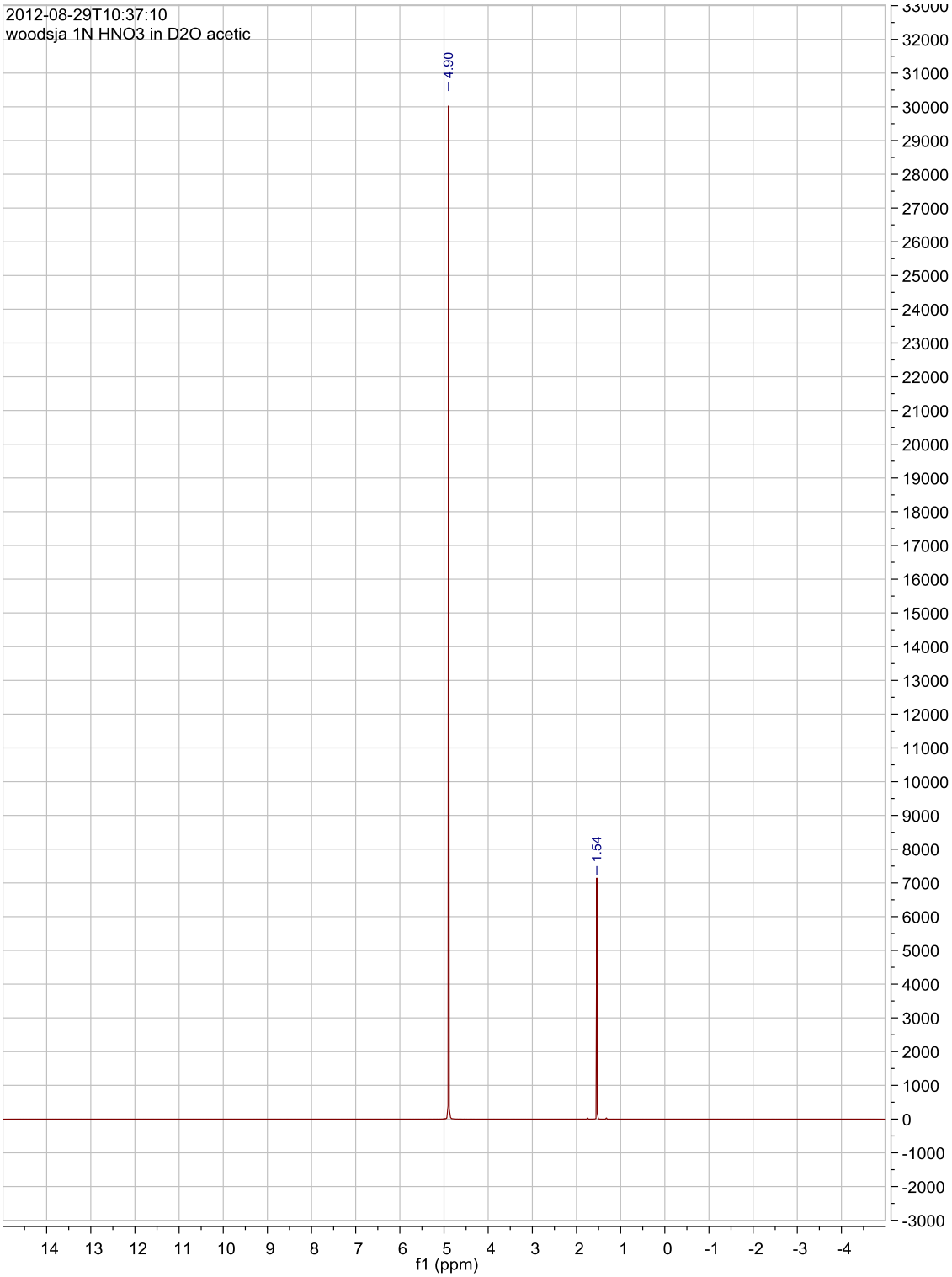

Figure S21: NMR spectrum of 1N HNO_3.in D_2O with 20 µL acetic acid

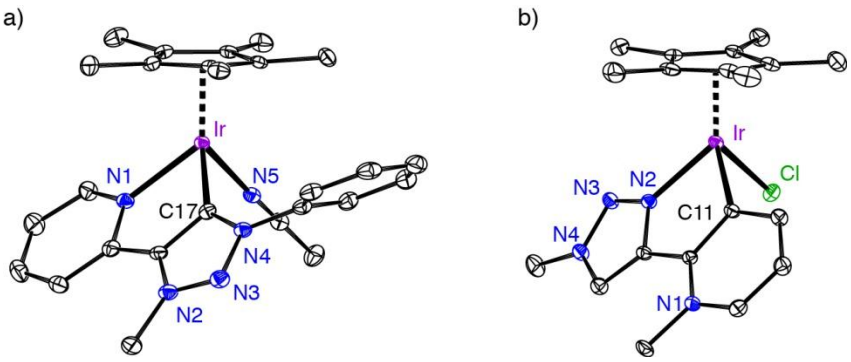

Figure S22. ORTEP plots of complexes **3** (a) and **6b** (b); structures at 50% probability level, hydrogen atoms, non-coordinating anions, and solvent molecules omitted for clarity.

Crystallographic Details:

Table S1. Crystal data and structure refinement for **1** (BPh_4 salt).

CCDC number	850694
Empirical formula	$C_{48}H_{47.38}BN_4O_{0.19}ClIr$
Molecular formula	$[C_{24}H_{27}N_4ClIr]^+[C_{24}H_{20}B]^- \times 0.19\ (H_2O)$
Formula weight	921.84
Temperature	100(2) K
Wavelength	0.71073 Å
Crystal system	Orthorhombic
Space group	Pbca (#61)
Unit cell dimensions	a = 16.8150(2) Å α= 90°.
	b = 17.5750(2) Å β= 90°.
	c = 28.6833(4) Å γ = 90°.
Volume	8476.59(18) $Å^3$
Z	8
Density (calculated)	1.445 Mg/m^3
Absorption coefficient	3.251 mm^{-1}
F(000)	3711.1
Crystal size	0.2632 x 0.1001 x 0.0333 mm^3
Theta range for data collection	3.30 to 24.79°.
Index ranges	$-19 \le h \le 19, -20 \le k \le 20, -33 \le l \le 33$
Reflections collected	134878
Independent reflections	7246 [R(int) = 0.0726]
Completeness to theta = 24.79°	99.5 %
Absorption correction	Analytical
Max. and min. transmission	0.906 and 0.645
Refinement method	Full–matrix least–squares on F^2
Data / restraints / parameters	7246 / 0 / 510
Goodness–of–fit on F^2	1.071
Final R indices [I>2sigma(I)]	R1 = 0.0217, wR2 = 0.0508
R indices (all data)	R1 = 0.0342, wR2 = 0.0526
Largest diff. peak and hole	0.917 and –0.707 $e.Å^{-3}$

Table S2. Crystal data and structure refinement for **3**.

CCDC number	850695
Empirical formula	$C_{20}H_{25}N_4O_3F_3SClIr$
Molecular formula	$[C_{19}H_{25}N_4ClIr]^+[CO_3F_3S]^-$
Formula weight	686.15
Temperature	100(2) K
Wavelength	0.71073 Å
Crystal system	Triclinic
Space group	P–1 (#2)
Unit cell dimensions	a = 8.1397(3) Å α= 93.308(2)°.
	b = 12.0802(4) Å β= 98.055(3)°.
	c = 12.1711(4) Å γ = 96.258(3)°.
Volume	1174.66(7) $Å^3$
Z	2
Density (calculated)	1.940 Mg/m^3
Absorption coefficient	5.940 mm^{-1}
F(000)	668
Crystal size	0.2045 x 0.1599 x 0.1138 mm^3
Theta range for data collection	3.39 to 29.79°.
Index ranges	$-11 \le h \le 11, -15 \le k \le 16, -16 \le l \le 16$
Reflections collected	31288
Independent reflections	6061 [R(int) = 0.0340]
Completeness to theta = 27.00°	99.6 %
Absorption correction	Analytical
Max. and min. transmission	0.583 and 0.443
Refinement method	Full–matrix least–squares on F^2
Data / restraints / parameters	6061 / 0 / 305
Goodness–of–fit on F^2	1.068
Final R indices [I>2sigma(I)]	R1 = 0.0206, wR2 = 0.0488
R indices (all data)	R1 = 0.0217, wR2 = 0.0494
Largest diff. peak and hole	2.742 and –1.729 e.$Å^{-3}$

Table S3. Crystal data and structure refinement for **4a**.

CCDC number	850692
Empirical formula	$C_{20}H_{25}N_4O_3F_3SClIr$
Molecular formula	$[C_{19}H_{25}N_4ClIr]^+[CO_3F_3S]^-$
Formula weight	686.15
Temperature	100(2) K
Wavelength	1.54184 Å
Crystal system	Monoclinic
Space group	$P2_1/n$ (#14)
Unit cell dimensions	a = 8.92686(6) Å α= 90°.
	b = 16.30625(8) Å β= 99.0197(5)°.
	c = 16.16290(9) Å γ = 90°.
Volume	2323.64(2) $Å^3$
Z	4
Density (calculated)	1.961 Mg/m^3
Absorption coefficient	13.517 mm^{-1}
F(000)	1336
Crystal size	0.2498 x 0.0872 x 0.0673 mm^3
Theta range for data collection	3.88 to 76.83°.
Index ranges	$-10 \le h \le 7, -20 \le k \le 20, -19 \le l \le 20$
Reflections collected	24544
Independent reflections	4734 [R(int) = 0.0167]
Completeness to theta = 76.83°	96.4 %
Absorption correction	Analytical
Max. and min. transmission	0.547 and 0.203
Refinement method	Full–matrix least–squares on F^2
Data / restraints / parameters	4734 / 0 / 306
Goodness–of–fit on F^2	1.105
Final R indices [I>2sigma(I)]	R1 = 0.0166, wR2 = 0.0421
R indices (all data)	R1 = 0.0170, wR2 = 0.0424
Extinction coefficient	0.000310(16)
Largest diff. peak and hole	0.480 and –0.678 $e.Å^{-3}$

Table S4. Crystal data and structure refinement for **4c**.

CCDC number	901533	
Empirical formula	$C_{21}H_{27}F_6IrN_4O_7S_2$	
Molecular formula	$[C_{19}H_{27}N_4OIr]^{2+}$ $2[CO_3F_3S]^-$	
Formula weight	817.79	
Temperature	100(2) K	
Wavelength	0.71073 Å	
Crystal system	Monoclinic	
Space group	$P2_1/c$ (#14)	
Unit cell dimensions	a = 11.2112(1) Å	α= 90°.
	b = 16.2011(2) Å	β= 90.907(1)°.
	c = 15.2890(2) Å	γ = 90°.
Volume	2776.65(6) $Å^3$	
Z	4	
Density (calculated)	1.956 Mg/m^3	
Absorption coefficient	5.047 mm^{-1}	
F(000)	1600	
Crystal size	0.2729 x 0.1946 x 0.0638 mm^3	
Theta range for data collection	2.85 to 29.44°.	
Index ranges	$-15 \le h \le 15$, $-21 \le k \le 22$, $-20 \le l \le 20$	
Reflections collected	60948	
Independent reflections	7261 [R(int) = 0.0261]	
Absorption correction	Analytical	
Max. and min. transmission	0.371 and 0.746	
Refinement method	Full–matrix least–squares on F^2	
Data / restraints / parameters	7261 / 0 / 383	
Goodness–of–fit on F^2	1.039	
Final R indices [I>2sigma(I)]	R1 = 0.0202, wR2 = 0.0397	
R indices (all data)	R1 = 0.0277, wR2 = 0.0423	
Largest diff. peak and hole	0.868 and –0.873 e.$Å^{-3}$	

Table S5. Crystal data and structure refinement for **5**.

CCDC number	850693
Empirical formula	$C_{52}H_{64}N_8OF_{12}P_2Cl_2Ir_2$
Molecular formula	$\{[C_{24}H_{27}N_4OClIr]^+[F_6P]^-\}_2 \times C_4H_{10}O$
Formula weight	1562.35
Temperature	100(2) K
Wavelength	0.71073 Å
Crystal system	Monoclinic
Space group	$P2_1$ (#4)
Unit cell dimensions	a = 8.6499(1) Å α= 90°.
	b = 30.9257(3) Å β= 95.343(1)°.
	c = 11.9013(2) Å γ = 90°.
Volume	3169.81(7) $Å^3$
Z	2
Density (calculated)	1.637 Mg/m^3
Absorption coefficient	4.405 mm^{-1}
F(000)	1532
Crystal size	0.1762 x 0.1408 x 0.0727 mm^3
Theta range for data collection	3.42 to 32.89°.
Index ranges	$-13 \le h \le 12$, $-46 \le k \le 46$, $-17 \le l \le 15$
Reflections collected	41286
Independent reflections	21125 [R(int) = 0.0277]
Completeness to theta = 30.00°	99.8 %
Absorption correction	Analytical
Max. and min. transmission	0.746 and 0.558
Refinement method	Full–matrix least–squares on F^2
Data / restraints / parameters	21125 / 45 / 725 [a)]
Goodness–of–fit on F^2	1.050
Final R indices [I>2sigma(I)]	R1 = 0.0350, wR2 = 0.0888
R indices (all data)	R1 = 0.0420, wR2 = 0.0902
Absolute structure parameter	0.478(5)
Largest diff. peak and hole	3.358 and –0.987 e.$Å^{-3}$

[a)] The ether molecule was restrained to have ideal shape using DFIX. ISOR and DELU restraints were applied to all non–hydrogen atom of the solvent.

Table S6. Crystal data and structure refinement for **6a**.

CCDC number	850699
Empirical formula	$C_{25}H_{27}N_4O_3F_3SClIr$
Molecular formula	$[C_{25}H_{27}N_4ClIr]^+[CO_3F_3S]^-$
Formula weight	748.22
Temperature	100(2) K
Wavelength	0.71073 Å
Crystal system	Monoclinic
Space group	$P2_1/n$ (#14)
Unit cell dimensions	a = 12.3897(3) Å α= 90°.
	b = 16.3148(3) Å β= 114.395(3)°.
	c = 14.6760(4) Å γ = 90°.
Volume	2701.69(13) $Å^3$
Z	4
Density (calculated)	1.840 Mg/m^3
Absorption coefficient	5.174 mm^{-1}
F(000)	1464
Crystal size	0.2591 x 0.1654 x 0.1327 mm^3
Theta range for data collection	3.29 to 29.84°.
Index ranges	$-16 \le h \le 17$, $-22 \le k \le 22$, $-16 \le l \le 18$
Reflections collected	23592
Independent reflections	6627 [R(int) = 0.0293]
Completeness to theta = 27.00°	99.3 %
Absorption correction	Analytical
Max. and min. transmission	0.587 and 0.439
Refinement method	Full–matrix least–squares on F^2
Data / restraints / parameters	6627 / 0 / 349
Goodness–of–fit on F^2	1.030
Final R indices [I>2sigma(I)]	R1 = 0.0210, wR2 = 0.0382
R indices (all data)	R1 = 0.0268, wR2 = 0.0403
Largest diff. peak and hole	0.821 and –0.604 e.$Å^{-3}$

Table S7. Crystal data and structure refinement for **6b**.

CCDC number	850698
Empirical formula	$C_{28}H_{30}N_5O_6F_6S_2Ir$
Molecular formula	$[C_{26}H_{30}N_5Ir]^{2+}\{[CO_3F_3S]^-\}_2$
Formula weight	902.89
Temperature	100(2) K
Wavelength	0.71073 Å
Crystal system	Monoclinic
Space group	$P2_1/n$ (#14)
Unit cell dimensions	a = 15.4068(2) Å α= 90°.
	b = 12.8634(1) Å β= 103.099(1)°.
	c = 17.5263(2) Å γ = 90°.
Volume	3383.05(6) $Å^3$
Z	4
Density (calculated)	1.773 Mg/m^3
Absorption coefficient	4.151 mm^{-1}
F(000)	1776
Crystal size	0.2305 x 0.1793 x 0.1190 mm^3
Theta range for data collection	3.38 to 30.04°.
Index ranges	$-20 \le h \le 21, -18 \le k \le 18, -24 \le l \le 23$
Reflections collected	37623
Independent reflections	9893 [R(int) = 0.0371]
Completeness to theta = 30.04°	99.8 %
Absorption correction	Analytical
Max. and min. transmission	0.694 and 0.506
Refinement method	Full–matrix least–squares on F^2
Data / restraints / parameters	9893 / 0 / 440
Goodness–of–fit on F^2	1.034
Final R indices [I>2sigma(I)]	R1 = 0.0252, wR2 = 0.0492
R indices (all data)	R1 = 0.0357, wR2 = 0.0532
Largest diff. peak and hole	2.007 and –0.726 e.$Å^{-3}$

Table S8. Crystal data and structure refinement for **7**.

CCDC number	850697
Empirical formula	$C_{32}H_{38}N_5O_7F_6S_2Ir$
Molecular formula	$[C_{27}H_{32}N_5Ir]^+\{[CO_3F_3S]^-\}_2 \times C_3H_6O$
Formula weight	974.99
Temperature	100(2) K
Wavelength	0.71073 Å
Crystal system	Monoclinic
Space group	$P2_1/c$ (#14)
Unit cell dimensions	a = 24.2752(3) Å α= 90°.
	b = 11.5628(1) Å β= 101.757(2)°.
	c = 27.0877(4) Å γ = 90°.
Volume	7443.71(16) $Å^3$
Z	8
Density (calculated)	1.740 Mg/m^3
Absorption coefficient	3.782 mm^{-1}
F(000)	3872
Crystal size	0.2465 x 0.1693 x 0.1275 mm^3
Theta range for data collection	3.33 to 31.08°.
Index ranges	$-35 \le h \le 35, -16 \le k \le 16, -37 \le l \le 39$
Reflections collected	106548
Independent reflections	23801 [R(int) = 0.0297]
Completeness to theta = 31.08°	99.6 %
Absorption correction	Analytical
Max. and min. transmission	0.664 and 0.512
Refinement method	Full–matrix least–squares on F^2
Data / restraints / parameters	23801 / 0 / 975
Goodness–of–fit on F^2	1.047
Final R indices [I>2sigma(I)]	R1 = 0.0353, wR2 = 0.0841
R indices (all data)	R1 = 0.0444, wR2 = 0.0895
Largest diff. peak and hole	4.328 and –1.362 e.$Å^{-3}$

Table S9. Crystal data and structure refinement for **8**.

CCDC number	850696
Empirical formula	$C_{24}H_{30}N_5O_6F_6S_2Ir$
Molecular formula	$[C_{22}H_{30}N_5Ir]^{2+}\{[CO_3F_3S]^-\}_2$
Formula weight	854.85
Temperature	100(2) K
Wavelength	0.71073 Å
Crystal system	Triclinic
Space group	P–1 (#2)
Unit cell dimensions	a = 9.9198(2) Å α= 88.964(2)°.
	b = 12.2357(3) Å β= 72.328(2)°.
	c = 14.1911(3) Å γ = 67.558(2)°.
Volume	1507.50(6) $Å^3$
Z	2
Density (calculated)	1.883 Mg/m^3
Absorption coefficient	4.652 mm^{-1}
F(000)	840
Crystal size	0.1696 x 0.1423 x 0.1143 mm^3
Theta range for data collection	3.36 to 33.15°.
Index ranges	$-15 \le h \le 15, -18 \le k \le 18, -21 \le l \le 21$
Reflections collected	96089
Independent reflections	10778 [R(int) = 0.0431]
Completeness to theta = 32.00°	99.2 %
Absorption correction	Analytical
Max. and min. transmission	0.700 and 0.576
Refinement method	Full–matrix least–squares on F^2
Data / restraints / parameters	10778 / 0 / 406
Goodness–of–fit on F^2	1.048
Final R indices [I>2sigma(I)]	R1 = 0.0172, wR2 = 0.0364
R indices (all data)	R1 = 0.0200, wR2 = 0.0374
Largest diff. peak and hole	1.115 and –0.928 e.$Å^{-3}$

Table S10. Crystal data and structure refinement for **11**.

CCDC number	850700
Empirical formula	$C_{30}H_{35}N_8O_6F_6S_2Ir$
Molecular formula	$[C_{28}H_{35}N_8Ir]^+\{[CO_3F_3S]^-\}_2$
Formula weight	973.98
Temperature	100(2) K
Wavelength	0.71073 Å
Crystal system	Monoclinic
Space group	$P2_1/c$ (#14)
Unit cell dimensions	a = 17.0427(7) Å α= 90°.
	b = 12.0904(5) Å β= 108.807(5)°.
	c = 18.0154(8) Å γ = 90°.
Volume	3513.9(3) $Å^3$
Z	4
Density (calculated)	1.841 Mg/m^3
Absorption coefficient	4.006 mm^{-1}
F(000)	1928
Crystal size	0.2135 x 0.1073 x 0.0228 mm^3
Theta range for data collection	3.37 to 24.18°.
Index ranges	$-18 \le h \le 19$, $-13 \le k \le 13$, $-20 \le l \le 20$
Reflections collected	28957
Independent reflections	5585 [R(int) = 0.0726]
Completeness to theta = 24.18°	99.3 %
Absorption correction	Analytical
Max. and min. transmission	0.902 and 0.607
Refinement method	Full–matrix least–squares on F^2
Data / restraints / parameters	5585 / 216 / 560
Goodness–of–fit on F^2	1.036
Final R indices [I>2sigma(I)]	R1 = 0.0362, wR2 = 0.0732
R indices (all data)	R1 = 0.0507, wR2 = 0.0798
Largest diff. peak and hole	1.558 and –1.006 e.$Å^{-3}$